Acoustic coupling to membrane waves on elastic shells

Andrew N. Norris and Douglas A. Rebinsky
Department of Mechanical and Aerospace Engineering, Rutgers University, Piscataway,
New Jersey 08855-0909

(Received 1 June 1993; accepted for publication 4 November 1993)

The interaction of an acoustic field with a smooth thin shell in a fluid is described by the superposition of a background field plus membrane waves on the shell. The former is defined by a local impedance condition, which accounts for the inertia of the shell, but takes no account of the in-surface, membrane effects. The shell's flexural stiffness turns out to be of secondary importance. The bulk of the paper deals with the coupling mechanism between the acoustic field and the supersonic membrane waves, both longitudinal and shear. The coupling is mediated by the shell curvature, and vanishes when the curvature vanishes. Ray methods are used to express the membrane waves by curved wave fronts with amplitudes subject to a transport equation over the curved shell surface. The coupling, and decoupling or launching, then reduces to solving an ordinary differential equation for the unknown ray amplitude. In essence, the transport equation is forced, or "beaten" by the locally phase-matched background field. Explicit expressions are obtained for the coupling and detachment coefficients on arbitrarily curved regions. These are combined, using ray theory for the propagation over the shell, to give the scattered field due to rays traveling over the shell. The general results are explicitly tested on the cylinder and sphere, for which the ensemble of surface rays can be summed into a resonance form, and numerical comparisons are made with the exact results for these canonical geometries.

PACS numbers: 43.20.Rk, 43.20.Fn, 43.30.Gv, 43.40.Rj

INTRODUCTION

Our purpose here is to present a theory that quantitatively describes the coupling mechanism whereby membrane waves are excited on and shed from elastic shells under heavy fluid loading. The central idea is that the supersonic, leaky membrane waves can be represented by ray methods as they travel over the shell, and their excitation occurs when the transport equation for the rays is forced by the incident field. In fact, as we will see, the forcing is through an intermediate, or background field, which accounts for the nonmembrane shell effects. The idea of a background field has been discussed recently in several articles, 1-5 including a paper by one of the present authors.6 In the latter work the additional field due to the membrane effects was represented by the global dry membrane modes of the structure. However, the present approach differs in that all membrane effects are explicitly local. Modes may be formed by combining rays, and examples of this will be presented for the canonical shapes, but our present emphasis is unambiguously on local, ravtype representations that are valid for arbitrary local surface geometry.

The motivation behind this work is the well-accepted notion that acoustic scattering from fluid-loaded elastic shells at high frequencies is most naturally viewed as a ray phenomenon. 7-11 In fact, most of our intuitive understanding of experimental data on acoustic scattering from complex structures is based upon ray concepts. 12 The present treatment of the membrane waves relies on recent work on ray equations for wave propagation over thin shells by Pierce, 13 Norris and Rebinsky, 14 and Norris; 15 see also

Refs. 16-19. At the same time we approximate the "background" field by a local impedance condition, 2,6 which results in a simple closed-form approximation for the specular field. We note that the ray point of view contrasts with the usual mathematical description of scattering in terms of a superposition of modes, although such an approach is perfectly natural in dealing with the separable targets—the cylinder and the sphere. A good review and an exhaustive list of references for scattering from the separable shells is provided by Gaunaurd and Werby. 20 The modal representation for these canonical shapes can be developed into a form that clearly displays the rays bouncing off the shell and traveling over its surface. 20 However, such global-tolocal analytical techniques (Poisson summation, Watson transform) are apparently limited to these two particular shapes.

The reader should keep in mind that the present analysis incorporates several simultaneous approximations—both physical and mathematical. The physical approximations may be grouped under the rubric of ray methods, with specific applications to non-Euclidean two-dimensional (2-D) spaces, i.e., curved surfaces. The associated mathematical "approximation" is to reduce the partial differential equations of the coupled fluid-structure system to ordinary differential equations (ODEs) along rays. The coupling mechanism then reduces to solving an inhomogeneous ODE for the ray amplitude on the shell (in fact, the ODE can be solved by explicit quadrature). The general framework is simplified by the use of "thin shell" theories that are physically valid only when the wavelengths of interest are much longer that the thickness h. At

the same time, we employ ideas from geometrical optics, requiring that the wavelengths be short in comparison with a typical radius of curvature, R. Both approximations may be justified from asymptotic arguments, but the asymptotics are in a sense conflicting. Unless we take the limit of $h/R \rightarrow 0$, it would be necessary to scale this ratio with the wavelength. One could proceed in this manner, but the complications would quickly hide the physical arguments. In summary, the methods proposed are primarily *physical*, and would be difficult to justify on purely formal, mathematical grounds. Some comments on these issues will be made later, but we emphasize that our philosophy here is to arrive at the simplest ray-theoretic description possible. Such issues as penumbral transitions,²¹ better shell theories, 2,22 interactions with discrete surface discontinuities, etc., could be included in the theory. However, these subjects are beyond the purview of this paper and will be discussed elsewhere.

The outline of the paper is as follows. We first deal with the 2-D case, as it illustrates the major features in the simplest manner. Section I describes the coupling and radiation mechanisms for membrane (longitudinal in 2-D) waves on arbitrarily curved 2-D shells. A formal asymptotic scaling is defined that illustrates the length scales of the coupling mechanism. The general theory is illustrated by application to the canonical case of a circular shell, for which comparison with an exact solution is possible. The fully three-dimensional case is discussed in Sec. II. The general theory treats an arbitrarily curved, smooth thin shell, and includes the possibility that the material properties (thickness, stiffness, etc.) are also smoothly varying. The physical principles are the same for the coupling and radiation as in two dimensions, but the added geometrical complexity of arbitrarily curved shells in three dimensions requires more algebra. Several new concepts are introduced, including the notion of a coupling curve along which membrane wave fronts are excited. Both longitudinal and shear waves are possible and must be considered simultaneously. We treat both wave types in parallel by introducing an effective curvature that determines the amount of coupling. For instance, the effective curvature for shear waves is proportional to the difference in principal curvatures of the surface, and hence vanishes on a spherical region. The main results of the 3-D analysis are summarized at the end of Sec. II. Several applications of the general theory are given in Sec. III, where numerical results are presented for the scattered fields predicted for the separable shapes, and comparisons are made with the exact solutions. Finally, we note that time harmonic motion is considered throughout, with the term $e^{-i\omega t}$ understood but suppressed.

I. TWO-DIMENSIONAL COUPLING

A. The asymptotic scaling and shell equations

An understanding of the local scattering phenomena is required to determine the coupling of an incident signal to the membrane waves on an arbitrary shell. We assume that the main excitation occurs at points on the structure at

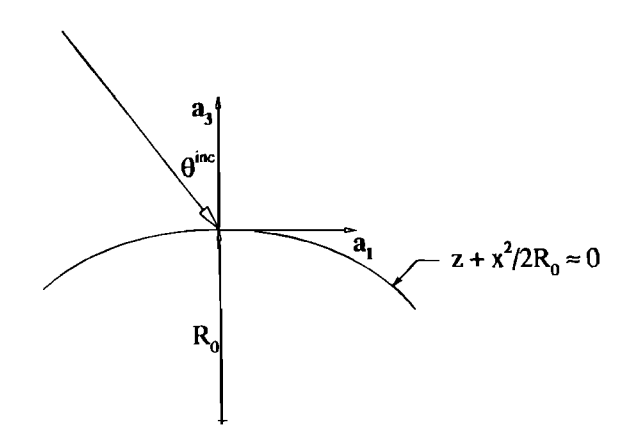


FIG. 1. The local coordinate system on the shell near the coupling point x=0.

which the incident wave is near the critical angle for the supersonic membrane wave. At such angles, the traditional geometric optics treatment of acoustic ray theory is inaccurate because of rapidly varying nonspecular behavior.²³ This is corrected by considering an inner or local problem in the neighborhood of these "coupling points" where the quickly varying signal is accounted for by a multiple scales analysis. The latter approach is motivated by a recent article by Tew and Ockendon²³ on the use of multiple scales to describe scattering from an impedance surface near the critical angle.

The supersonic, leaky membrane wave in the shell is assumed to have complex-valued surface wave number $k=k_f\sin\theta_s$, where $k_f=\omega/c_f$ is the fluid acoustic wave number, and the angle θ_s is complex, but only slightly so. Define the real angle θ_0 by

$$\sin \theta_s = \sin \theta_0 + i\delta, \quad \delta > 0, \tag{1}$$

where $\delta < 1$. The fact that δ is small means that the surface wave is only weakly radiating, or leaky. Now consider a plane wave incident at angle $\theta^{\rm inc}$ with the local normal to the shell. The incident wave reflects in a normal or "specular" manner when $\theta^{\rm inc} \neq \theta_0$ but if $\theta^{\rm inc} \approx \theta_0$ then coupling occurs and a membrane wave is excited. We assume, for simplicity, a 2-D situation, such that the shell has a locally parabolic shape at the point of incidence, given as $z+x^2/2R_0\approx 0$, where R_0 is the radius of curvature at that point (see Fig. 1). Define a small parameter

$$\epsilon = 1/k_f R_0, \tag{2}$$

such that $k_f R_0 > 1$ by assumption. The local analysis is valid for incident waves near the critical angle, which occurs if $\theta^{\text{inc}} - \theta_s = O(\epsilon^{1/2})$ or, specifically,

$$\sin \theta^{\rm inc} = \sin \theta_s + \sqrt{\epsilon} \Lambda, \tag{3}$$

where $\Lambda = O(1)$. Also, let the coupling point coincide with the origin, and consider positions x such that $k_f / \epsilon x = O(1)$. Now define the slow scale through the dimensionless position vector:

$$\mathbf{X} = \sqrt{\epsilon} \mathbf{k}_f \mathbf{x}.\tag{4}$$

We will be concerned with the "inner region" where X=O(1).

Scaling the frequency is a rather delicate issue for thin shells, on account of the multitude of characteristic frequencies at our disposal: specifically, the ring, null, coincidence, and Poisson frequencies. For a shell of radius R_0 and thickness $h \ll R_0$, the ring frequency is a low-frequency parameter associated with the fundamental membrane mode, and occurs at $k_f = c_p/c_f R_0$, where c_p is the longitudinal plate wave speed. The null frequency,²⁴ at $k_f = \rho_f/\rho h$, where ρ_f and ρ are the fluid and solid densities, provides a rough separation between the lowfrequency, heavy-fluid-loading regime in which the shell acts more like a pressure release surface, and higher frequencies where fluid loading is weak and the surface is more like a rigid target.^{2,6} The coincidence frequency defines the transition of the flexural wave on a flat plate from subsonic to supersonic, and is given by = $(c_f/c_p)\sqrt{12/h}$. The Poisson frequency, introduced by Kaplunov et al., is, like the ring frequency, a membrane frequency that depends upon the shell curvature. However, it is a high-frequency local (as opposed to global) parameter that defines the frequency where the exterior pressure effects the membrane shell equations directly. This results in a membrane forcing proportional to the in-surface gradient of the pressure and proportional to the Poisson's ratio.^{2,22} Such effects are ignored in most shell theories, including those used here, which are based directly upon the work of Green and Zerna²⁵ and coincide with other shell theories commonly used, e.g., Ref. 19. Kaplunov et al.² have shown that for a sphere of radius R_0 the Poisson frequency occurs at $k_f = (c_p/c_f) \sqrt{(1-v^2)/vhR_0}$ (the value $k_f = x_0/R_0$ in the notation of Ref. 2), where ν is the Poisson's ratio of the plate. Note that the Poisson frequency becomes infinite as the Poisson effect vanishes $(\nu \rightarrow 0)$. It helps to consider a specific example. All of the calculations in this paper are for steel shells in water, with $R_0/h=90$, $c_f=1482$, $c_p=5435$, $\rho_f=1000$, $\rho=7800$, and ν =0.289, all in mks units. The value of the dimensionless frequency $k_f R_0$ at the ring, null, Poisson, and coincidence frequencies is then 3.67, 11.6, 62.0, and 85.0, respectively.

In this paper we are concerned with the membrane coupling effect in the midfrequency range, which is defined as the range of frequencies between the ring and Poisson frequencies. At the same time, we assume that the coincidence frequency lies outside this range (above it), hence allowing us to ignore bending effects in the shell equations and thus simplifying the analysis. The midfrequency range specifically includes the null frequency, so that fluidloading effects are critical. In practice, this means that the "background" response is neither that of a rigid or a soft surface, but is truly intermediate.2 We assume that the midfrequency range is large in the sense that we may use the geometrical optics limit $k_1R_0 > 1$, but at the same time we have the additional constraint of thin shell theory, i.e., that $h/R_0 < 1$. These conditions are met for the example of the steel shell in water with $R_0/h=90$ if we consider the midfrequency range to be defined roughly as $5 < k_f R_0 < 60$. At the lower end of the range the geometrical optics assumptions break down, while at the high end we encounter discrepancies arising from the simplicity of the shell theory used here. One could probably push the upper limit of applicability to higher values through the use of more sophisticated shell theories.²²

Let s be the arclength on the shell near the point of interest, and v(s) and w(s) be the in-surface and normal components, respectively. The shell is approximated locally as a parabolic surface described by the equations of motion for a thin cylindrical shell with equivalent radius of curvature. The final approximated local form of the equations of motion are

$$\frac{d^2v}{ds^2} + k_p^2 v + \frac{1}{R_0} \frac{dw}{ds} = 0, (5a)$$

$$\frac{1}{R_0}\frac{dv}{ds} - k_p^2 w = \frac{-p}{C},\tag{5b}$$

where $k_p = \omega/c_p$, c_p is the longitudinal plate velocity, and C is the extensional stiffness. See Appendix A for further details. The local equations (5) follow from the 3-D equations for a cylindrical thin shell [Eqs. (A2)] by neglecting bending effects $(\beta \rightarrow 0)$ and the term w/a^2 in the w equation (A2c).

In addition, the continuity condition for timeharmonic motion is

$$\rho_f \omega^2 w = \frac{\partial p}{\partial n},\tag{6}$$

where ρ_f is the fluid density and n is the normal to the surface S. At this stage we introduce some impedances that enter into many of the subsequent formulas:

$$Z_m = -i\omega\rho h$$
, $Z_s = \rho_f c_f \sec \theta_s$, $Z_f(\theta) = \rho_f c_f \sec \theta$. (7)

Thus, Z_m is the masslike impedance of the shell, Z_s is the local impedance for a membrane surface wave, and $Z_f(\psi)$ is the impedance that will enter into geometrical optics approximations for specularly reflection. We note that $Z_s = Z_f(\theta_s) \approx Z_f(\theta_0)$.

B. The background wave field

We first determine the outer or background solution, which consists of inertial effects on the shell and produces the specular reflection into the fluid for angles of incidence away from the critical, i.e., $\theta^{\rm inc} \neq \theta_s$. It is also the driving mechanism for the inner or local problem, when $\theta^{\rm inc} \approx \theta_s$ in the sense of Eq. (3). We are mainly interested in the midfrequency regime defined above, and therefore flexural effects are ignored; in fact, we have explicitly expunged them from the shell equations (5). Consider the ansatz

$$p = p^{(0)} + \epsilon p^{(1)} + \cdots,$$
 (8a)

$$w = w^{(0)} + \epsilon w^{(1)} + \cdots,$$
 (8b)

$$v = \epsilon v^{(0)} + \epsilon^2 v^{(1)} + \cdots$$
 (8c)

Note that the v displacement is scaled to be smaller than the pressure and the normal displacement. Upon substitu-

tion into Eq. (5b), one obtains the leading-order approximations for the w equation as

$$i\omega Z_m w^{(0)} = p^{(0)},$$
 (9)

where Z_m is defined in (7). Combined with the leadingorder contribution to the continuity equation (6), Eq. (9) results in a local impedance boundary condition on the surface S.

$$\frac{\partial p^{(0)}}{\partial n} + \frac{i\omega \rho_f}{Z_m} p^{(0)} = 0. \tag{10}$$

This local impedance condition has been previously derived and discussed by Norris and Vasudevan⁶ and by Kaplunov, Nolde, and Veksler. Equation (10), together with the Helmholtz equation.

$$\nabla^2 p^{(0)} + k_p^2 p^{(0)} = 0, \tag{11}$$

defines the background field or outer solution $p^{(0)}$ in the surrounding volume V. This is the response with no coupling to the longitudinal membrane wave.

The background pressure $p^{(0)}$ is composed of the sum of the incident and scattered wave fields, $p^{(0)} = p^{\text{inc}} + p^{\text{sc}(0)}$. We assume an incident wave field in the fluid in the form of a curved wave front or a Gaussian beam, which has local paraxial form²⁶

$$p^{\text{inc}}(\mathbf{x}) = P_0 \exp\{ik_f[\mathbf{n}^{\text{inc}} \cdot \mathbf{x} + \frac{1}{2}M_0(\mathbf{m}^{\text{inc}} \cdot \mathbf{x})^2]\}, \quad (12)$$

where P_0 is the amplitude, M_0 is the wave-front curvature (which could be complex valued), and $\mathbf{n}^{\text{inc}} = \sin \theta^{\text{inc}} \mathbf{a}_1 - \cos \theta^{\text{inc}} \mathbf{a}_3$ and $\mathbf{m}^{\text{inc}} = \mathbf{a}_2 \wedge \mathbf{n}^{\text{inc}}$ are unit vectors. Here, {a1,a2,a3} form a right-handed orthonormal triad (see Fig. 1 for a description of the local coordinates). The background scattered field $p^{sc(0)}$ in the surrounding fluid may be written in a geometrical optics form similar to the incident wave field (12), i.e., as a curved wave front or Gaussian beam [assuming the incident curvature satisfies $M_0R_0=O(1)$:

$$p^{sc(0)}(\mathbf{x}) = P_0^{sc} \exp\{ik_f[\mathbf{n}^{sc} \cdot \mathbf{x} + \frac{1}{2}M_0^{sc}(\mathbf{m}^{sc} \cdot \mathbf{x})^2]\},$$
 (13)

where $n^{sc} = \sin \theta^{inc} a_1 + \cos \theta^{inc} a_3$ and $m^{sc} = a_2 \wedge n^{sc}$. Equation (13) is local in the sense that the amplitude and curvature are independent of position. This is all that is required for our purposes, but we note that one could use geometrical optics²⁶ to analytically continue $p^{sc(0)}$ to the far field. The reflected amplitude and wave-front curvature are given by

$$P_0^{\rm sc} = \mathcal{R}(\theta^{\rm inc}) P_0, \quad M_0^{\rm sc} = M_0 + 2/(R_0 \cos \theta_s),$$
 (14)

where

$$\mathcal{R}(\theta) = [Z_m - Z_f(\theta)] / [Z_m + Z_f(\theta)]. \tag{15}$$

In summary, the background wave field $p^{(0)}$ is described by the incident pressure of Eq. (12), plus the scattered pressure of Eqs. (13)-(15). The displacement $w^{(0)}$ can be determined using Eq. (9). The specular approximation of Eqs. (14) and (15) is consistent with the more general equations of Kachalov, 21 who derived specular and penumbral approximations using a more general local shell

impedance function that includes bending effects. We prefer to keep the background field as simple as possible, partially to explore the extent to which flexural effects are significant. As we will see, very good approximations can be attained with this simple background response.

C. Generation of the membrane wave

We now consider the inner solution that describes the behavior of the shell when the incident field couples to the longitudinal membrane wave. As the membrane wave travels supersonically along the shell energy is constantly leaked back into the surrounding fluid, interfering with the reflected wave field generated by the outer solution discussed above. The total wave field produced in the surrounding fluid, with both background and membrane wave components, changes significantly in magnitude and phase with position when the angle of incidence θ^{inc} is near the critical angle $\theta_{...}$

A different approximation is required to include coupling to the longitudinal wave. The leading-order solution is represented as a sum of the background solution plus an additional component generated by the longitudinal wave. This additional component will be referred to as the inner solution. We assume, for simplicity, that the shell material properties are uniform for X=O(1), and start with the ansatz

$$p = p^{(0)} - i\omega Z_s F\Phi(X) e^{ik_f m \cdot x} + \cdots, \qquad (16a)$$

$$w=w^{(0)}+F\Phi(X)e^{iks}+\cdots, \qquad (16b)$$

$$v = \Phi(\mathbf{X})e^{iks} + \cdots, \tag{16c}$$

where the inner solution consists of an unknown amplitude function Φ dependent upon the slow variable X multiplied by a phase that varies according to the fast variable x. Note that $\Phi(X)$ has an argument that can be both in the fluid and on the surface, although it is understood that the shell displacements are only defined on S. The impedance Z_s of (7) appears in Eq. (16a) by virtue of the fact that this is the impedance appropriate to the membrane wave, and the vector $\mathbf{m} = \sin \theta$, $\mathbf{a}_1 + \cos \theta$, \mathbf{a}_3 . At this stage we do not scale Φ with ϵ , although it will transpire that $\Phi = O(\sqrt{\epsilon})$.

The coefficient F may be found by substituting the above response into the w equation (5b). Note that in the local region the arclength s is reasonably approximated by x and that the normal derivative is the z component to leading order. Using the fact that the background solution satisfies Eq. (9), an algebraic equation is obtained to leading order for the coefficient F, giving

$$F \approx i\epsilon_s [Z_m/(Z_m + Z_s)]. \tag{17}$$

This approximation uses the fact that $\sin \theta_s \approx c_f/c_n$, and the definition [see Eq. (2)] $\epsilon_s = 1/kR_0 \approx \epsilon \csc \theta_0$. The pressure solution given by Eq. (16a) must also satisfy the Helmholtz equation, which governs the response in the surrounding fluid. Upon substitution of Eq. (16a), one obtains

$$\nabla^2 p + k_f^2 p = -2\omega k_f^2 \sqrt{\epsilon} Z_s F e^{ik\mathbf{m} \cdot \mathbf{x}} \mathbf{m} \cdot \nabla_{\mathbf{X}} \Phi + O(\epsilon) = 0.$$
(18)

Therefore, to $O(\sqrt{\epsilon})$,

$$\mathbf{m} \cdot \nabla_{\mathbf{X}} \Phi(\mathbf{X}) = 0, \tag{19}$$

which means that Φ must be a function only of the component $(\mathbf{a}_2 \wedge \mathbf{m}) \cdot \mathbf{X}$. Noting that $(\mathbf{a}_2 \wedge \mathbf{m}) \cdot \mathbf{X} = X \cos \theta_s$, we write the general solution as

$$\Phi(\mathbf{X}) = \bar{\Phi}(\sec \theta_s(\mathbf{a}_2 \wedge \mathbf{m}) \cdot \mathbf{X}) = \bar{\Phi}(\mathbf{X}). \tag{20}$$

The amplitude function $\bar{\Phi}$ is determined from the condition that there is no forcing of the longitudinal wave on the surface S. Thus, with the form of the F known, substitute the inner response given by Eqs. (16) into the vequation (5a), yielding

$$(k_{p}^{2}-k^{2})\bar{\Phi}(X)+2ik_{f}k\sqrt{\epsilon}\frac{d\bar{\Phi}(X)}{dX}+\cdots +\frac{1}{R_{0}}\frac{dw^{(0)}}{dx}e^{-ikx}+\frac{F}{R_{0}}ik\bar{\Phi}(X)+\frac{F}{R_{0}}k_{f}\sqrt{\epsilon}\frac{d\bar{\Phi}(X)}{dX}=0.$$
(21)

The terms linear in $\bar{\Phi}$ vanish because of the dispersion relation satisfied by the surface wave number; or alternatively, k is determined by the vanishing of its coefficient. Setting the latter to zero and using (17) to approximate Fyield the dispersion relation

$$k^2 \approx k_p^2 - \frac{Z_m}{Z_m + Z_s} \frac{1}{R_0^2}$$
 (22)

The second term on the right-hand side is asymptotically smaller than the first, but it introduces the crucial complex part to k, associated with the radiation loss into the fluid.

The remaining terms in Eq. (21) imply

$$\left(1 + \frac{F}{2ikR_0}\right) 2ik \frac{d\overline{\Phi}(X)}{dX} = -\sqrt{\epsilon} \frac{dw^{(0)}}{dx} e^{-iks}, \text{ on } S.$$
(23)

The term in parentheses may be replaced by unity without any significant error because $F/2ikR_0$ is of $O(\epsilon^2)$, from Eq. (17). The outer solution for $w^{(0)}$ is required to determine the amplitude function of the inner solution, $\bar{\Phi}$. In general circumstances, $w^{(0)}$ is composed of contributions from the direct incident wave plus, possibly, flexural waves that have traveled to the point of interest from some distance source on the shell. Such waves could be common on complex structures where discontinuities act as sources and the flexural waves could, in theory, influence points far away on the structure because they propagate subsonically and therefore suffer no radiation loss. However, for our purposes we can safely ignore any flexural wave contributions to the $w^{(0)}$, since they are out of phase with the membrane wave and their presence in the right member of Eq. (23) would have an insignificant effect in exciting the membrane wave. By the same reasoning, we may safely replace $w^{(0)}$ by the part of the normal displacement that is excited directly, or locally, by the incident acoustic wave. The phase is then approximately matched, so that to a good approximation $dw^{(0)}/dx = ikw^{(0)}$, and Eq. (23) then reduces to

$$\frac{d\bar{\Phi}(X)}{dX} = -\frac{\sqrt{\epsilon}}{2} w^{(0)} e^{-iks}.$$
 (24)

The outer contribution to $w^{(0)}$ follows from Eq. (9), using the background pressure fields of Eqs. (12) and (13),

$$w^{(0)} = \frac{(P_0 + P_0^{\text{sc}})}{i\omega Z_m} \exp(ikx) \exp\left[i\left(\Lambda X + \frac{1}{2}\hat{M}_0 X^2\right)\right],$$
on S, (25)

where

$$\hat{M}_0 = \cos \theta_s + \bar{M}_0 \cos^2 \theta_s. \tag{26}$$

After substitution of Eq. (25) into Eq. (24), using Eq. (15), the inner solution amplitude function is found to be

$$\vec{\Phi}(X) = \frac{\sqrt{\epsilon}}{-i\omega} \frac{P_0}{Z_m + Z_s} \int_{-\infty}^{X} \exp\left[i\left(\Lambda S + \frac{1}{2}\hat{M}_0 S^2\right)\right] dS$$

$$= \frac{\sqrt{\epsilon}}{-i\omega} \frac{P_0}{Z_m + Z_s} \sqrt{\frac{2}{\hat{M}_0}} e^{-i\Lambda^2/2\hat{M}_0}$$

$$\times \int_{-\infty}^{\sqrt{\hat{M}_0/2}(X + \Lambda/\hat{M}_0)} e^{iS^2} dS, \qquad (27)$$

where the lower limit of integration is chosen to satisfy the radiation condition.²³ The integral in Eq. (27) has the form of a complex error function, which can be written in terms of Fresnel integrals. However, the behavior of the integral can be best surmised by examining what happens as the upper limit of integration tends to $\pm \infty$ $(X \rightarrow \pm \infty)$, for which the integral becomes

$$\sqrt{\pi}e^{i\pi/4}H(X) + \frac{\exp[(i/2)\hat{M}_0(X + \Lambda/\hat{M}_0)^2]}{i\sqrt{2\hat{M}_0}(X + \Lambda/\hat{M}_0)} + \cdots,$$
(28)

where H is the Heaviside step function. The first term of Eq. (28) denotes the supersonic membrane wave traveling along the surface of the shell in the local region, and the other term describes the modifications to the (outer) specular field. For intermediate values of X the integral provides a smooth, although oscillatory, transition region in which the membrane wave is created.²³

The leading term of Eq. (28) provides the coupling coefficient or the initial amplitude of the generated surface membrane wave. Thus, the amplitude of the longitudinal wave traveling along the shell's surface is $\Phi \rightarrow \Phi_{surf}$, where

$$\Phi_{\text{surf}} = \frac{\sqrt{\epsilon}}{-i\omega} \frac{P_0}{Z_m + Z_s} \sqrt{\frac{2\pi i}{\hat{M}_0}} e^{-i\Lambda^2/2\hat{M}_0}.$$
 (29)

Referring to the ansatz (8), we see that the in-surface displacement is $O(\sqrt{\epsilon})$, in contrast to $O(\epsilon)$ for the outer solution. Thus the "beating" of the acoustic wave, combined with the shell curvature, results in an enhanced tangential displacement, which in turn launches a membrane wave. The simplest case is that of an incident plane wave,

for which $M_0=0$. The exponential term in Eq. (29) introduces a decay unless the angle of incidence is $\theta=\theta_0$. Assuming that $\theta=\theta_0$, the surface wave amplitude for a plane wave reduces to

$$\Phi_{\text{surf}} \approx \frac{\sqrt{\epsilon}}{-i\omega} \frac{P_0}{Z_m + Z_s} \sqrt{\frac{2\pi i}{\cos \theta_0}}.$$
 (30)

Note that the amplitude is $O(\sqrt{\epsilon})$, as compared to the smaller $O(\epsilon)$ of Eq. (8c) for the background in-surface response. The in-phase beating of the membrane wave therefore induces a coherent response of magnitude $O(\epsilon^{-1/2})$ relative to the background, and dominates the in-surface response.

D. Coupling from the shell to the fluid

The coefficient describing the amount of coupling to the membrane wave was calculated in the previous subsection, and provides the initial condition for the generated surface wave. As the membrane wave travels along the shell its energy is shed into the surrounding fluid through radiation leakage. The resulting attenuation is described by the imaginary part of the membrane wave number k. In order to determine the response in the surrounding fluid, in particular the energy that "leaks" to the far field, the Helmholtz equation must be satisfied with the pressure along the surface appropriate to a membrane wave. Accordingly, we start with the following surface fields, which are based upon the inner solution of Eqs. (16):

$$\{p, w, v\} = \{-i\omega Z_s F, F, 1\} V_0 e^{iks}, \text{ on } S,$$
 (31)

where V_0 is an arbitrary amplitude with dimension of length. The field in the surrounding fluid may be determined by applying Green's theorem,

$$p(\mathbf{x}') = \int_{S} \left(G \frac{\partial p}{\partial n} - p \frac{\partial G}{\partial n} \right) ds, \tag{32}$$

where G is the 2-D free-space Green's function, $G(\mathbf{x},\mathbf{x}') = (-i/4)H_0^{(1)}(k_f|\mathbf{x}-\mathbf{x}'|)$, and the normal in (32) is exterior to the empty shell. Using the boundary values of (31), Eq. (32) becomes

$$p(\mathbf{x}') = i\omega Z_s F V_0 \int_S e^{iks} \left(\frac{\partial G}{\partial n} - ik_f \cos \theta_s G \right) ds.$$
 (33)

Consider the configuration shown in Fig. 2, with $\mathbf{x'} = R' \sin \theta \, \mathbf{a}_1 + R' \cos \theta \, \mathbf{a}_3$. We assume that the dominant contribution to the radiated field originates from points on the surface S for which \mathbf{x} lies in the neighborhood of the origin. Then,

$$|\mathbf{x} - \mathbf{x}'| \approx R' - x \sin \theta + (\cos \theta / R_0 + \cos^2 \theta / R') x^2 / 2$$

while Eq. (33) and the large argument approximation for G imply

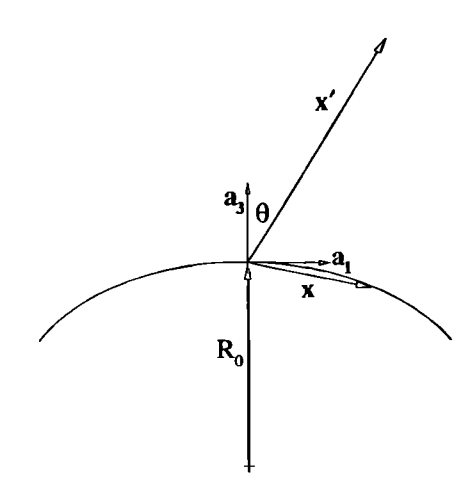


FIG. 2. The configuration and location of the coordinate system for the launching of a wave from a point x on the surface to some position x' in the far field.

$$p(\mathbf{x}') \approx \omega k_f Z_s F V_0(\cos \theta + \cos \theta_s) G(0, \mathbf{x}') \int d\mathbf{x}$$

$$\times \exp\left[ik_f \left[(\sin \theta_s - \sin \theta) \mathbf{x} + \left(\frac{\cos \theta}{R_0} + \frac{\cos^2 \theta}{R'}\right) \frac{\mathbf{x}^2}{2} \right] \right]. \tag{34}$$

The integral can be evaluated by the method of stationary phase and has an exponential term of the form

$$\exp\left[-\frac{i}{2}k_f(\sin\theta_s - \sin\theta)^2 \left[\left(\frac{\cos\theta}{R_0} + \frac{\cos^2\theta}{R'}\right)\right]^{-1}\right],\tag{35}$$

which is exponentially small unless $\theta = \theta_0$, where θ_0 is defined in (1). Hence, the main contribution to the radiated wave field from the region near $\mathbf{x} = 0$ lies in the direction $\theta = \theta_0$, and follows from (34). This simplifies in the far field $(R' \gg R_0)$ to

$$p(\mathbf{x}') \approx G(0,\mathbf{x}') 2i\omega \cot \theta_0 \sqrt{\epsilon} V_0 \left(\frac{1}{Z_m} + \frac{1}{Z_s}\right)^{-1} \sqrt{\frac{2\pi i}{\cos \theta_0}}.$$
(36)

The approximation $\sin \theta_0 \approx c_f/c_p$ has been used here. Note the similarity of this expression to that for the launch coefficient in Eq. (30).

Combining Eqs. (30) and (36) allows us to compute the contribution to the scattering from membrane waves for arbitrary incidence. For example, suppose the incident field originates from a point source at \mathbf{x}' , couples to the membrane wave at \mathbf{x}_1 on S, and radiates from \mathbf{x}_2 , also on S, to the field point \mathbf{x} . For simplicity, we assume that both the source and receiver are in the far field (their distance greatly exceeds the radii of curvature). Along the surface between the coupling points, the amplitude of the membrane wave goes as $1/\sqrt{\rho c_p h(s)}$, if the shell parameters vary smoothly between $s=s_1$ and $s=s_2$ at \mathbf{x}_1 and \mathbf{x}_2 . Otherwise it remains constant, although there is some inevitable decay resulting from the fact that k has a small positive

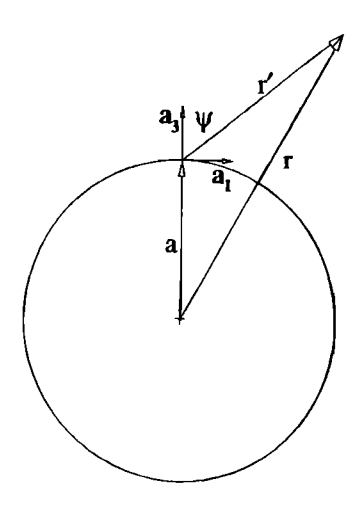


FIG. 3. Circular cylindrical shell with coordinate system, source direction, and observation point locations.

imaginary part. Combining all these results, we find that the radiated response due to the membrane wave is

$$p(\mathbf{x}) \approx G(\mathbf{x}', \mathbf{x}_1) G(\mathbf{x}_2, \mathbf{x}) D_1 D_2 \exp\left(i \int_{s_1}^{s_2} k \, ds\right),$$
 (37)

where the "diffraction" coefficients are defined by

$$D = i \frac{(4\pi \rho c_p Z_s)^{1/2}}{Z_m + Z_s} \sqrt{\frac{h}{R_0}}.$$
 (38)

Note the phase term due to the launch and scattering, in addition to the phase from the propagation over the shell. Also, the result (37) is clearly the same under the interchange of the source and receiver points, as required by reciprocity. Suppose, for simplicity, that the shell is uniform between the launch and radiating points, with arclength of L separating them. If the incident plane wave is of amplitude P_0 at the launch point, then the scattered field is

$$p(\mathbf{x}) \approx \frac{-i4\pi}{kR_0} \frac{Z_m Z_s}{(Z_m + Z_s)^2} P_0 G(\mathbf{x}_2, \mathbf{x}) e^{ikL}.$$
 (39)

We next use this simple result to test the theory on the 2-D circular shell.

E. Example: The cylindrical shell

We consider an incoming plane wave scattered by a circular cylinder of radius a. For this canonical geometry, $R_0 = a$ and the exact far-field scattering amplitude can be determined and compared with that obtained from the ray description. The far-field scattering amplitude is defined by

$$\mathcal{F} = \lim_{r \to \infty} \left[\sqrt{2r/a} e^{-ik_f r} (p - p^{\text{inc}}) \right], \tag{40}$$

where r is measured from the center of the cylinder to the far field (see Fig. 3). The coordinate system is now placed at the center of the cylinder as opposed to that used in the previous calculations where it was located on the surface of the shell at the location of each incident ray.

Recall that the total response consists of an interaction between the specularly reflected wave field with that shed by the leaky membrane wave traveling along the cylinder's surface. The former follows from Eq. (13), yielding

$$p^{\text{sc}(0)} = P_0 \mathcal{R}(\psi) [1 + 2r'/(a\cos\psi)]^{-1/2}$$

$$\times \exp[ik_f(r' - a\cos\psi)], \tag{41}$$

where

$$r' = -a\cos\psi + \sqrt{r^2 - a^2\sin\psi},\tag{42}$$

and the impedance $Z_f(\psi)$ is defined in Eq. (7). Next, the leaky membrane waves are described by Eq. (39) with the arclength between the launch and radiating points L to be determined. If the far-field scattering amplitude is calculated on the clockwise (cw) side of the cylinder than the arclengths traveled by the membrane waves traveling counterclockwise and clockwise are $2a(\pi-\psi-\theta_0)$ and $2a[\pi H(\theta_0 - \psi) + \psi - \theta_0]$, respectively, where H is the Heaviside function. Each wave circumnavigates the cylinder continuously giving an additional arclength of $2\pi a$ per cycle, and their contributions to the phase in Eq. (39) can be written as

$$\sum_{m=0}^{\infty} e^{ik2\pi am} = \frac{1}{1 - e^{i2\pi ka}},$$
 (43)

where the complex-valued surface wave number k is determined from Eq. (22). Then, the radiated response of the total contribution of the leaky membrane waves is

$$p^{\text{mem}} = -P_0 \frac{4\pi}{ka} \frac{Z_m Z_s}{(Z_m + Z_s)^2} \frac{e^{ik_f (r' - a\cos\theta_0)}}{\sqrt{8\pi i k_f r'}} \frac{1}{1 - e^{i2\pi ka}}$$

$$\times \{e^{i2ka[\pi H(\theta_0 - \psi) + \psi - \theta_0]} + e^{i2ka(\pi - \psi - \theta_0)}\}. \tag{44}$$

Now the far-field scattering amplitude given by Eq. (40) is evaluated using Eqs. (41), (42), and (44) to obtain

$$-\frac{4}{ka}\sqrt{\frac{\pi}{ik_{f}a}}\frac{Z_{m}Z_{s}}{(Z_{m}+Z_{s})^{2}}e^{-i2k_{f}a\cos\theta_{0}}\frac{e^{ika(\pi-2\theta_{0})}}{1-e^{i2\pi ka}}$$

 $\mathcal{F} = \sqrt{\cos \psi} \mathcal{R}(\psi) e^{-i2k_f a \cos \psi}$

$$\times \begin{bmatrix} \cos[ka(\pi-2\psi)], & \psi > \theta_0, \\ \cos(2ka\psi)e^{i\pi ka}, & \psi \leqslant \theta_0, \end{bmatrix}$$
(45)

where \mathcal{F} has been normalized with respect to the incident wave-field amplitude and a phase shift corresponding to the diameter of the cylinder. The term in curly braces in p^{mem} has been rearranged in the above to illustrate better the behavior at the resonances occurring when ka is almost equal to an integer. Note that the membrane wave expression (44) and its contribution to (45) are both discontinuous at $\psi = \theta_0$. This nonuniformity arises from the simple ray summation used. One could modify these expressions to account for the uniform transition that occurs as ψ passes θ_0 , associated with the smooth "turn-on" of a mem-

The far-field scattering amplitude predicted by the above asymptotic formulas is compared in Fig. 4 with the exact calculation for the thin shell equations of Appendix

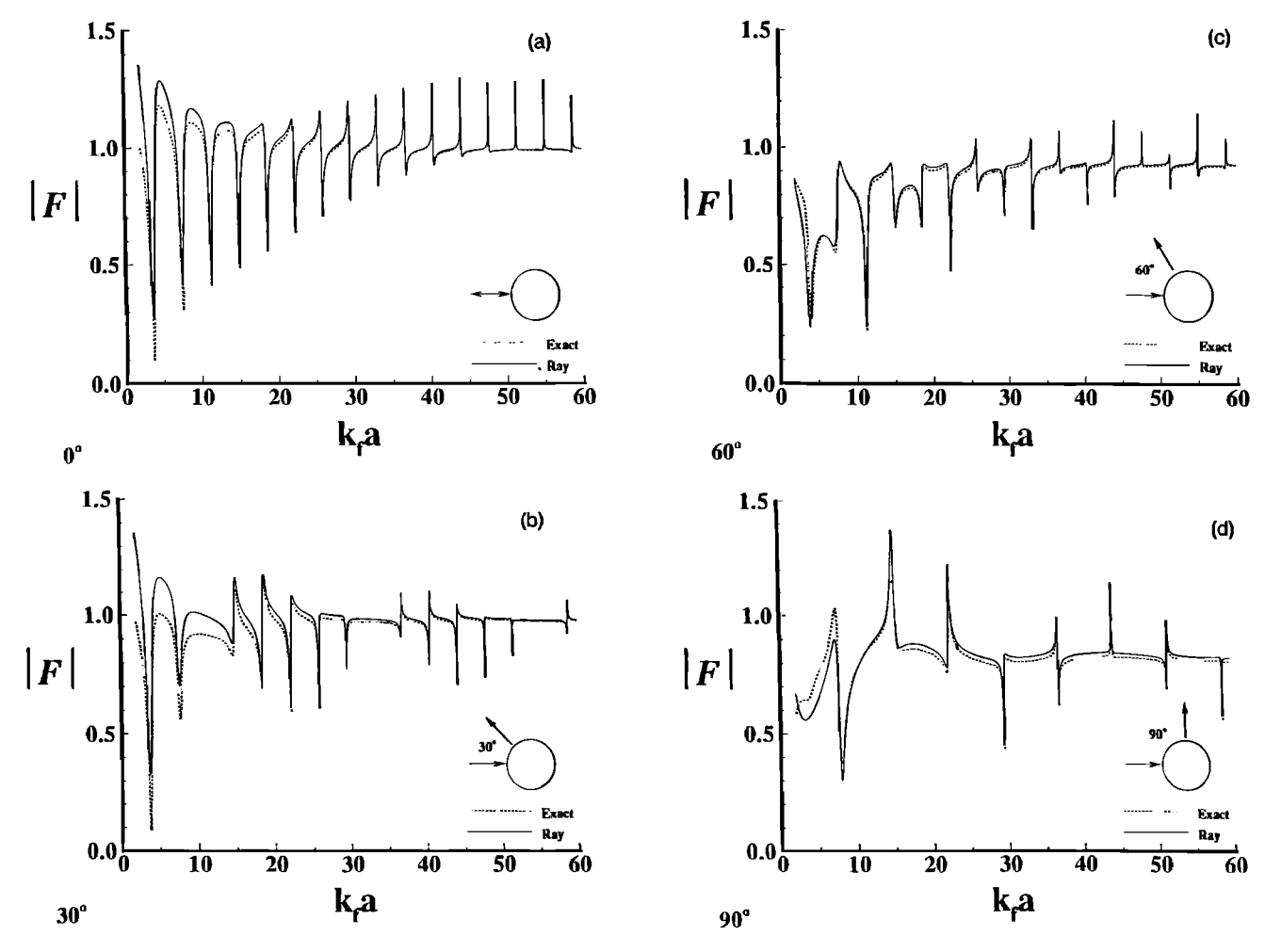


FIG. 4. Comparison of exact and ray-based form functions for a circular cylindrical shell with broadside plane wave incidence. The different observation directions are (a) 0°, (b) 30°, (c) 60°, and (d) 90°. Note that the agreement improves with increasing k₁a. As the observation angle increases, the ray theory overestimates because of the simple approximation used for the specular wave field.

A. The parameters used in these and later calculations are for a steel shell in water (see Sec. I A). We note that the asymptotic theory accurately predicts the locations of the resonances for the midfrequency regime. For small values of $k_{i}a_{i}$, the inaccurate prediction of the asymptotic theory is not unexpected since it is based upon a high-frequency ansatz, although the qualitative agreement is still good. Also, as the scattering angle increases from 0° (the backscatter direction), the discrepancy in the mean level prediction increases, which may be ascribed to the simple form chosen for the specularly reflected field. It is evident from Fig. 4 that some of the resonances disappear as the scattering angle increases from 0°. In the second term of Eq. (45), the numerator may also be equal to zero for some of the resonances. After applying l'Hôpital's rule, the behavior of this term can be described by $\sin(2n\psi)$, where n is an integer value of ka. Therefore, the second term is zero for $2n\psi/\pi$. For example, when the scattering angle is 30°, every sixth resonance disappears in the far-field scattering amplitude in comparison to that obtained for backscatter.

II. THREE-DIMENSIONAL THEORY

There are two major areas of complication in going from two to three dimensions. First, the geometrical details are that much harder, and, of course, the shell dynamics are more sophisticated. Therefore, some geometrical concepts need to be introduced before considering the shell equations and the coupling mechanism.

A. Local geometry at the coupling point

We begin by describing the surface S near the point x_0 at which the incident pressure phase matches the membrane wave, whether longitudinal or transverse. Let n be the surface direction vector of the membrane ray produced "at" x_0 . We will consider the most general case of a smooth but arbitrarily curved and inhomogeneous shell in the neighborhood of x_0 . The vector n subsequently follows a ray path n=n(s), where s is the ray arclength. The surface ray can be calculated by integration of the ray equation, as discussed by Norris. 15 Let r be the coordinate for curves orthogonal to the ray, in the direction $n^1 \equiv a_1 \wedge n$. The directions of principal curvature at x_0 are denoted by \mathbf{a}_{1} and $\mathbf{a}_{11} = \mathbf{a}_{3} \wedge \mathbf{a}_{1}$, with principal radii of curvature R_{1} and $R_{\rm II}$ and principal coordinates $\theta^{\rm I}$ and $\theta^{\rm II}$. We also consider general curvilinear coordinates θ^1 and θ^2 on the shell, with corresponding direction vectors $\mathbf{a}_{\alpha} \equiv \mathbf{x}_{,\alpha}$, $\alpha = 1,2$, and normal $a_3 = a_1 \wedge a_2 / |a_1 \wedge a_2|$ directed out of the shell. Greek sub- or superscripts assume the values 1 or 2, and the suffix α denotes differentiation with respect to θ^{α} . The surface metric and curvature tensors are $a_{\alpha\beta} = \mathbf{a}_{\alpha} \cdot \mathbf{a}_{\beta}$, and $d_{\alpha\beta} = \mathbf{a}_{\alpha} \cdot \mathbf{a}_{3,\beta}$, respectively. The local form of the surface near \mathbf{x}_0 may be written

$$\mathbf{x} = \mathbf{x}_{0} + \theta^{\alpha} \mathbf{a}_{\alpha} - \frac{1}{2} d_{\alpha\beta} \theta^{\alpha} \theta^{\beta} \mathbf{a}_{3} + \cdots$$

$$= \mathbf{x}_{0} + \theta^{I} \mathbf{a}_{I} + \theta^{II} \mathbf{a}_{II} - \frac{1}{2} \left(\frac{(\theta^{I})^{2}}{R_{I}} + \frac{(\theta^{II})^{2}}{R_{II}} \right) \mathbf{a}_{3} + \cdots$$

$$= \mathbf{x}_{0} + s\mathbf{n} + r\mathbf{n}^{\perp} - \frac{1}{2} \left(\frac{s^{2}}{R_{\parallel}} + \frac{r^{2}}{R_{\perp}} + \frac{2sr}{R_{\perp}} \right) \mathbf{a}_{3} + \cdots, \quad (46)$$

where the first form is general, the second is in terms of the principal coordinates, and the final is in terms of the ray coordinates, $(\theta^1, \theta^2) \rightarrow (s,r)$, with

$$\frac{1}{R_{\parallel}} = \frac{n_{\rm I}^2}{R_{\rm I}} + \frac{n_{\rm II}^2}{R_{\rm II}},\tag{47a}$$

$$\frac{1}{R_{\rm I}} = \frac{n_{\rm II}^2}{R_{\rm I}} + \frac{n_{\rm I}^2}{R_{\rm II}},\tag{47b}$$

$$\frac{1}{R_T} = n_{\rm I} n_{\rm II} \left(\frac{1}{R_{\rm II}} - \frac{1}{R_{\rm I}} \right),\tag{47c}$$

where $n_{\rm I}$ and $n_{\rm II}$ are the components of n in the principal directions. Thus, R_{\parallel} and R_{\perp} are the normal radii of curvatures of the surface for curves parallel and perpendicular to n.

B. The coupling point and the coupling curve

We will need to match the incident phase to the surface wave on S. The paraxial approximation to the incident phase is $\phi^{\rm inc} = k_f(\mathbf{n}^{\rm inc} \cdot \mathbf{x} + \frac{1}{2}\mathbf{x} \cdot \mathbf{M} \cdot \mathbf{x})$, where $\mathbf{n}^{\rm inc}$ is the incident central ray direction at \mathbf{x}_0 . The incident wave-front curvature is defined by \mathbf{M} , which could be complex valued, but is symmetric with $\mathbf{M} \cdot \mathbf{n}^{\rm inc} = 0$. The Snell condition for the incident ray is

$$\mathbf{n}^{\text{inc}} = \sin \theta_0 \,\mathbf{n} - \cos \theta_0 \,\mathbf{a}_3. \tag{48}$$

The incident phase becomes, using (46) and (48),

$$\phi^{\text{inc}} = k \left[s + \frac{1}{2} \cot \theta_0 \left(\frac{s^2}{R_{\parallel}} + \frac{r^2}{R_{\perp}} + \frac{2sr}{R_T} \right) + \frac{1}{2} \csc \theta_0 \mathbf{x} \cdot \mathbf{M} \cdot \mathbf{x} \right], \quad \text{on } S.$$
(49)

For simplicity, the remaining analysis is based on the assumption that the incident field is a plane wave, so that M=0.

The incident wave also couples to the membrane wave at other points in the neighborhood of \mathbf{x}_0 . In order to find these points and their locus, we note that the normal to S is locally approximated by $\mathbf{a}_3' = \mathbf{a}_3 + d_\beta^a \theta^\beta \mathbf{a}_\alpha$, which can also be expressed in terms of the principal and ray coordinate systems. The coupling condition for a plane wave is basically that $\mathbf{n}^{\text{inc}} \cdot \mathbf{a}_3' = -\cos \theta_0$. Applying this in the neighborhood and using the condition that \mathbf{x}_0 is a coupling point, and Eq. (48), we deduce that the nearby points must satisfy

$$d_{\alpha\beta}n^{\alpha}\theta^{\beta} = 0, (50)$$

or, equivalently,

$$\frac{s}{R_{\parallel}} + \frac{r}{R_{T}} = 0 \quad \text{or} \quad \frac{n_{\text{I}}}{R_{\text{I}}} \theta^{\text{I}} + \frac{n_{\text{II}}}{R_{\text{II}}} \theta^{\text{II}} = 0, \tag{51}$$

in ray coordinates and principal coordinates, respectively. This equation defines the local tangent to the coupling curve. A global differential equation for the coupling curve could be easily constructed by analytically continuing (50); however, we will only examine the local tangent to the curve at x_0 . If one of the principal curvatures vanishes, then it is clear that the coupling curve is locally parallel to that principal direction. An important example of this is when S is a developable surface, such as a cone or cylinder, which has zero Gaussian curvature at all points, $1/R_1R_{11}=0$. The coupling curves are always parallel to the directions of zero curvature on these surfaces. In general, the curvature of the coupling curve is given by $1/R_C = d^{\alpha\beta} m_\alpha m_\beta$, where m is the unit tangent vector to the curve. A simple calculation gives

$$R_{C} = R_{\rm I} R_{\rm II} \left(\frac{n_{\rm I}^{2}}{R_{\rm I}^{2}} + \frac{n_{\rm II}^{2}}{R_{\rm II}^{2}} \right) \left(\frac{n_{\rm I}^{2}}{R_{\rm I}} + \frac{n_{\rm II}^{2}}{R_{\rm II}} \right)^{-1}.$$
 (52)

The curvature $1/R_C$ vanishes at points on the shell which have zero local Gaussian curvature. Hence, it vanishes at every point on a cone or a cylinder, or any developable surface.

C. Thin shell equations and background field

Before dealing with the coupling to membrane waves we first summarize the shell equations used. The full set of equations for an inhomogeneous, isotropic shell are ^{13,19}

$$C^{-1}\nabla_{\beta}\{C[(1-\nu)e^{\alpha\beta}+\nu e^{\gamma}_{\gamma}a^{\alpha\beta}]\}+k_{p}^{2}v^{\alpha}=0, \quad \alpha=1,2,$$
(53a)

$$\Gamma + (1 - v)d_{\beta}^{\alpha}e_{\alpha}^{\beta} + vd_{\alpha}^{\alpha}e_{\beta}^{\beta} - k_{p}^{2}w = -p/C,$$
 (53b)

with

$$\Gamma = C^{-1} \nabla_{\alpha} \nabla_{\beta} \{ (h^2/12) C[(1-\nu) a^{\alpha\lambda} a^{\beta\gamma} \nabla_{\lambda} \nabla_{\gamma} w + a^{\alpha\beta} \nu \Delta w] \}, \tag{54}$$

where ∇_{α} denotes the covariant derivative, and $\Delta = a^{\alpha\beta}\nabla_{\alpha}\nabla_{\beta}$ is the surface Laplacian. The displacement vector of a point originally on the middle surface is decomposed into tangential and normal components as $\mathbf{u} = v^{\alpha}\mathbf{a}_{\alpha} + w\mathbf{a}_{3}$, and the in-surface strains are $e_{\alpha\beta} = (a_{\beta\gamma}\nabla_{\alpha}v^{\gamma} + a_{\alpha\gamma}\nabla_{\beta}v^{\gamma})/2 + d_{\alpha\beta}w$. The parameter $C \equiv Eh/(1-v^{2})$ is the extensional stiffness, where E is the Young's modulus, and v is the Poisson's ratio of the shell material. Also, the longitudinal plate wave speed is $c_{p}^{2} = C/\rho h$ and for future reference, the transverse wave speed is $c_{t} = c_{p}\sqrt{(1-v)/2}$. These equations are supplemented by the continuity condition (6) on S and the Helmholtz equation for the pressure in the exterior fluid.

The approximate 2-D equations (5) follow quite easily from Eqs. (53) by dropping the term Γ involving the bending stiffness. We will neglect this term also in the 3-D

analysis. This approximation is justified by a separate analysis of membrane waves¹⁴ and by restricting the frequency to lie below the coincidence frequency. 6 We return to this point later, but note that it results in a simpler system at this stage, which is the natural generalization of the 2-D system (5). The ansatz for the background wave field is again given by (8) with the generalization $v \rightarrow v^{\alpha}$. This implies that the in-surface displacements decouple, and we again obtain Eq. (9). Thus, the background field satisfies the relatively simple impedance boundary condition (10).

D. Coupling to membrane waves

The scaled position X and a slowly varying amplitude function $\Phi(X)$ were used in the 2-D analysis. In the present 3-D analysis we will work directly with x without recourse to a slow scale. This simplifies the equations, but it makes the distinctions between the fast and slow dependencies less obvious. We will see that the equation that generalizes (24) is a forced transport equation for the amplitude of the membrane wave.

1. The membrane wave

The ansatz for p, w, and the in-surface displacement is similar to the previous one [Eqs. (16)], but for the sake of simplicity we will only look at the fields on the surface. The pressure can be continued into the fluid quite easily. We

$$\begin{vmatrix} v^{\alpha} \\ w - w^{(0)} \\ p - p^{(0)} \end{vmatrix} = V(s)e^{i\phi} \begin{cases} q^{\alpha}, \\ F(s), \\ -i\omega Z_{s}(s)F(s), \end{cases}$$
 (55)

where q is the normalized polarization vector of the membrane wave; q=n for longitudinal waves, and $q=n^{\perp}$ for transverse waves. Also, ϕ is the surface phase function, which defines the surface wave number k,

$$k_{\alpha} \equiv \nabla_{\alpha} \phi = k n_{\alpha}. \tag{56}$$

Thus, n is the phase direction of the membrane wave. The amplitude factor F follows from Ref. 14 as

$$F = \frac{i}{kR_0} \frac{Z_m}{Z_m + Z_s} \approx \frac{i}{2kR_0} \left[1 + \mathcal{R}(\theta_0) \right], \tag{57}$$

where now R_0 is an effective local radius of curvature at the launch point, given by

$$\frac{1}{R_0} = \begin{cases} 1/R_{\parallel} + \nu/R_{\perp}, & \text{longitudinal,} \\ 2/R_T, & \text{transverse.} \end{cases}$$
 (58)

The dispersion relation for the fluid loaded membrane waves is

$$k^2 \approx \frac{\omega^2}{c^2} + \frac{1 - v}{R_1 R_{11}} - \frac{Z_m}{Z_m + Z_s} \frac{1}{R_0^2},$$
 (59)

where $c=c_p$ for longitudinal waves, and $c=c_t$ for transverse waves. The asymptotic results [(57)-(59)] follow by applying ray theory to the general shell equations and looking for solutions that are predominantly in-surface. The method is outlined below, and details are given by Norris and Rebinsky, 14 who discuss all except the term

 $(1-\nu)/R_IR_{II}$. This term is of second order, because by assumption the wave number far exceeds the curvature in magnitude. It can be obtained by regrouping higher-order terms with the leading-order terms in the asymptotic formalism of Norris and Rebinsky,14 and is discussed elsewhere. 15 We retain the term here because it turns out to provide a better approximation to the dispersion relation at low frequencies for the spherical shell example discussed in

The solution given by Eq. (55) evolves according to ray theory in the absence of the applied forcing from $p^{(0)}$ and $w^{(0)}$, in which case the phase ϕ can be described by the paraxial approximation. This requires tracing the ray on S and solving the wave-front curvature along the ray path. The ray amplitude V(s) evolves according to the transport equation, which in turn depends upon the wavefront curvature. The ansatz (55) assumes a similar type of solution, except that the amplitude is now driven by the external forcing, but only over a finite region. Outside that region the unforced transport equation takes over.

2. The eikonal equation

Substituting (55) into the in-surface equilibrium equations (53a) and defining the in-surface amplitude components

$$V^{\alpha} = Vq^{\alpha} \tag{60}$$

give

$$\begin{aligned} \{k_{p}^{2}V^{\alpha} - (k^{2}/2)[(1+v)n^{\alpha}n_{\beta}V^{\beta} + (1-v)V^{\alpha}] \\ + ikF\widetilde{d}_{\beta}^{\alpha}V^{\beta}\} + iC^{-1}\nabla_{\beta}(C\{[(1-v)/2]] \\ \times (k^{\alpha}V^{\beta} + k^{\beta}V^{\alpha}) + vk_{\gamma}V^{\gamma}a^{\alpha\beta}\}) + ivk^{\alpha}\nabla_{\beta}V^{\beta} \\ + i[(1-v)/2](k^{\beta}\nabla_{\beta}V^{\alpha} + k^{\beta}a^{\alpha\lambda}\nabla_{\lambda}V_{\beta}) \\ + e^{-i\phi}\widetilde{d}^{\alpha\beta}\nabla_{\beta}w^{(0)} + \dots = 0, \end{aligned}$$

$$(61)$$

where $d_{\beta}^{\alpha} = (1 - v)d_{\beta}^{\alpha} + vd_{\gamma}^{\gamma}a_{\beta}^{\alpha}$. The first term in parentheses determines the wave number k. Setting it to zero, contracting with q_{α} , and dividing by V give

$$(k^2/2)[1-\nu+(1+\nu)(n_{\beta}q^{\beta})^2] = k_p^2 + ikF\tilde{d}^{\alpha\beta}n_{\beta}q_{\alpha}.$$
(62)

Substituting q=n and $q=n^1$ and using Eqs. (57) and (58) then imply the dispersion relation (59), except for the term discussed above, which requires including higherorder contributions. 15 It should be admitted that these q vectors are not precise eigenvectors of the matrix occurring in the first parenthetical term in (61), except if F=0 or n coincides with a principal direction. However, the contribution from F is implicitly assumed to be small, so that these eigenvectors are correct to first order. Standard perturbation analysis then implies that the dispersion relation is correct to second order. We include the additional two terms [see Eq. (59)] in the dispersion relation because the fluid-loading, or F, term provides an attenuating mechanism (through radiation loss) where there is otherwise none, and the second provides a better approximation, as we will see in the examples. However, we omit these terms

from the transport and ray equations, as their absence simplifies these considerably. The former omission is analogous to our previously dropping the F term in Eq. (23), while the latter is justified by the expectation that the fluid loading and anisotropy does not appreciably alter the ray paths, or that the dispersion is appreciable. Conditions under which these assumptions are invalid have been discussed by Norris and Rebinsky. The dispersive and anisotropic terms could be included, but at the expense of all the attendant complications associated with these phenomena. Therefore, we emphasize that the ray theory considered here is *isotropic* and *nondispersive*.

3. The transport equation

Contraction of the remaining terms in Eq. (61) with V_{α} followed by some simplification gives the forced transport equation

$$\nabla_{\beta} \{ (C/2) \left[(1-\nu)k^{\beta}V^{2} + (1+\nu)k^{\alpha}V_{\alpha}V^{\beta} \right] \}$$

$$= iCe^{-i\phi}V^{\alpha}\widetilde{d}_{\alpha}^{\beta}\nabla_{\beta}w^{(0)}. \tag{63}$$

Following the arguments given in the 2-D analysis, this equation can be simplified by first assuming that the outer field satisfies $\nabla_{\alpha}w^{(0)} \approx ik_{\alpha}w^{(0)}$. The right member of (63) then simplifies considerably using Eqs. (58) and (60). Further reduction results from approximating k as $k \approx \omega/c$ in the right member, where $c=c_p$ or c_t , while the left member simplifies by again using Eq. (60). Also, noting that $C=\rho hc_p^2$ and $C(1-\nu)/2=\rho hc_t^2$, Eq. (63) reduces to

$$\frac{\omega}{c}\frac{d}{ds}\left(\rho hc^{2}V^{2}\right) + \rho hc^{2}V^{2}\Delta\phi = -\omega\rho hc\frac{V}{R_{0}}w^{(0)}e^{-i\phi}.$$
(64)

Before proceeding any further we need to define and evaluate the term $\Delta \phi$.

Referring to Norris, ¹⁵ the ray equation for membrane waves or the evolution equation for the vector $\mathbf{n} = \mathbf{n}(s)$, where $n^{\alpha} = d\theta^{\alpha}/ds$, is

$$\frac{dn^{\alpha}}{ds} + \Gamma^{\alpha}_{\beta\gamma}n^{\beta}n^{\gamma} + n^{\perp\alpha}n^{\perp\beta}\frac{c_{\beta}}{c} = 0.$$
 (65)

This reduces to the equation for geodesics on S if c is constant. The paraxial approximation to the phase along a ray on a curved surface is

$$\frac{1}{\omega} \nabla_{\alpha} \nabla_{\beta} \phi = \frac{1}{Ac} \frac{dA}{ds} n_{\alpha}^{\downarrow} n_{\beta}^{\downarrow} - n^{\downarrow \lambda} \frac{c_{,\lambda}}{c^{2}} (n_{\alpha} n_{\beta}^{\downarrow} + n_{\alpha}^{\downarrow} n_{\beta})$$

$$- n^{\lambda} \frac{c_{,\lambda}}{c^{2}} n_{\alpha} n_{\beta}. \tag{66}$$

Here A(s) is the ray tube area parameter along the ray, and its evolution equation is¹⁵

$$c\frac{d}{ds}\frac{1}{c}\frac{dA}{ds} + \left(\frac{1}{R_{\rm I}R_{\rm II}} + \frac{1}{c}n^{\perp \alpha}n^{\perp \beta}\nabla_{\alpha}\nabla_{\beta}c\right)A = 0.$$
 (67)

We note that the two terms in the parentheses induce nonlinear ray spreading, in the sense that rays diverge linearly with distance in uniform, Euclidean space (see Ref. 15 for a complete discussion). Taking the trace of Eq. (66) gives $\Delta \phi = (\omega/A)d(A/c)/ds$, which allows us to rewrite Eq. (64), after some simplification, as a linear differential equation for the amplitude,

$$\frac{d}{ds}\left(V\sqrt{\rho hcA}\right) = -\frac{1}{2}\sqrt{\rho hcA}\frac{w^{(0)}}{R_0}e^{-i\phi}.$$
 (68)

This is the desired coupling equation; but it cannot be solved in ignorance of A(s), for which we need to prescribe initial conditions for A(0) and its derivative A'(0).

4. The phase matching

Equation (68) provides us with an equation for the evaluation of the ray amplitude V(s). Before integrating it we must address two related issues: (i) the phase ϕ , and (ii) the initial conditions for A(s). The general form of ϕ follows from Eqs. (56) and (66) and simplifies in regions of constant c to

$$\phi(s) = k \left(s + \frac{r^2}{2A(s)} \frac{dA}{ds} \right). \tag{69}$$

Thus, the paraxial phase is a function of s alone. Referring to Eq. (49) we see that ϕ^{inc} , and, hence, the phase of the right member in Eq. (68), can depend upon both s and the transverse coordinate r. However, by hypothesis V is a function of s only, and therefore its ODE should not depend upon r.

This difficulty of matching the incident phase locally to the phase of a Gaussian beam, or curved wave front, does not arise in all situations. For instance, when a plane wave strikes a spherical shell the principal directions for the incident phase function coincide with the ray and transverse directions. In general, we must deal with the possibility of terms involving sr in Eq. (49), which would arise, for instance, on an ellipsoidal surface. The occurrence of these phase terms means that the incident phase, although not locally in the form of a curved wave front on the surface, is eventually "beaten" into such a form. We circumvent this issue by replacing the phase of the right member of Eq. (68) with one that depends only upon s. Specifically, we take

$$w^{(0)}e^{-i\phi} \approx w^{(0)}(\mathbf{x}_0)\exp\left(ik\frac{\cot\theta_0}{R_{\parallel}}\frac{s^2}{2}\right).$$
 (70)

At the same time, the initial conditions for A are taken as

$$A(0) = 1, \quad \frac{d}{ds} \left(\frac{A}{c}\right)(0) = \frac{\cot \theta_0}{c} \frac{R_{\parallel}}{R_{\rm I} R_{\rm II}}.$$
 (71)

As justification for Eqs. (70) and (71) we offer the following arguments. Suppose we try to simply replace the phase of the incident wave with one of the form

$$\phi^{\rm inc} \to k \left[s + \frac{1}{2} \cot \theta_0 \left(\frac{s^2}{R_A} + \frac{r^2}{R_B} \right) \right], \tag{72}$$

for some R_A and R_B . Then, in order that this new field produce the correct "beating" along the ray axis, r=0, we must take $R_A=R_\parallel$, from Eq. (49). We next obtain a condition for R_B by requiring that the determinant of the second derivatives of the new phase be the same as the orig-

inal, i.e., $R_A R_B = R_I R_{II}$. This implies $R_B = R_I R_{II} / R_{\parallel}$, which is equivalent to the initial conditions (71). We note that the initial condition for A(0) is still arbitrary and is chosen as A(0) = 1 for simplicity. The initial condition for dA/ds then follows from (69) and the value of R_B . An alternative and more rigorous justification for Eqs. (70) and (71) is given in Appendix B, which compares the final form of V(s) that results from these equations with the amplitude determined using the shell Green's function.

5. The coupling equation

Having found the initial conditions for the ray tube area, we can now obtain the coupling equation. Substituting (70) into (68) and then integrating subject to the initial condition that $V(-\infty)=0$ give

$$V(s) = \frac{-w^{(0)}(\mathbf{x}_0)}{2\sqrt{\rho h c A(s)}} \int_{-\infty}^{s} \frac{\sqrt{\rho h c A}}{R_0} \exp\left(ik \frac{\cot \theta_0}{R_{\parallel}} \frac{s'^2}{2}\right) ds'.$$
 (73)

This is the *coupling equation*. The ray tube area A(s) is determined separately by integrating Eq. (67) subject to the initial conditions (71).

The coupled wave amplitude (73) may be written in terms of the incident pressure amplitude P_0 instead of the displacement amplitude $w^{(0)}(\mathbf{x}_0)$. The relationship between these quantities is analogous to that for the 2-D theory, from Eqs. (15) and (25), and is easily shown to be

$$w^{(0)}(\mathbf{x}_0) = \{ [1 + \mathcal{R}(\omega_0)] / i\omega Z_m \} P_0. \tag{74}$$

We have kept the ray tube area and other parameters within the integral in Eq. (73) to include the possibility that these all vary along the ray. However, such variation can be neglected in the limit of very high frequency, in which case we can ignore the dependence of the preexponential term on s. The coupled wave amplitude follows by letting $s \to \infty$. Using (74) we find

$$V(s) \to \frac{-P_0}{i\omega k R_0} \frac{(i2\pi k R_{\parallel} \tan \theta_0)^{1/2}}{Z_m + Z_s} \left(\frac{\rho h c A(0)}{\rho h c A(s)}\right)^{1/2}.$$
(75)

This is the 3-D version of the 2-D result (30), which can be seen to follow from (75).

One could improve on this high-frequency limit by taking into account the initial spreading of the rays. For example, consider the approximation $A(s) \approx A(0) + sA'(0)$. This linear rate of spreading is exact on surfaces of zero Gaussian curvature, although the initial spreading rate, A'(0), which is given by (71), is identically zero on such surfaces. The curvature $1/R_A$ is not zero on spherical surfaces, but in this particular case the equation for A(s) is harmonic and the linear approximation to A(s) is just that, an approximation. Suppose for simplicity that the shell properties are uniform, and we assume further that R_0 is constant. Then, using the linear approximation for A(s), the general integral (73) reduces to

$$V(s) = \frac{-w^{(0)}(\mathbf{x}_0)}{2R_0 \sqrt{A(s)}} \times \int_{-w^{(0)}}^{s} \sqrt{1 + \frac{z \cot \theta_0}{R_A}} \exp\left(ik \frac{\cot \theta_0}{R_{\parallel}} \frac{z^2}{2}\right) dz.$$
 (76)

This could be further simplified using parabolic cylinder functions, but we will not pursue this further here. The lower limit in the integral is in quotation marks to reflect the fact that it does not include the fictitious focus of the linearized A at $s=-R_A \tan\theta_0$, although we can set the limit as $-\infty$ with no loss in accuracy. The coupling integral in Eq. (76) reflects the fact that the surface disturbance has a nonzero wave-front curvature that changes in the "beating" region. However, in the limit of very high frequency this region shrinks and any spreading on the surface is insignificant, in which case (75) is once again recovered.

E. Coupling from the shell to the fluid

The analysis is similar to that for the 2-D case. We consider the launching of membrane wave from a point x_0 on the surface. The local form of the variables $\{p, w, v^a\}$ on the surface follow from Eq. (55), which compares with the 2-D version (31). Applying Green's theorem we obtain the following representation for the radiation:

$$p(\mathbf{x}') = i\omega \int_{S} Z_{s}(s) F(s) V(s) e^{i\phi(s,r)}$$

$$\times \left(\frac{\partial G}{\partial n} - ik_{f} \cos \theta_{s} G\right) dS, \tag{77}$$

where the 3-D free-space Green's function is $G(\mathbf{x},\mathbf{x}') = -\exp(ik_f|\mathbf{x}-\mathbf{x}'|)/4\pi|\mathbf{x}-\mathbf{x}'|$. Note that the integral in (77) is over the surface, although the ray approximation to the membrane wave is parameterized by the ray coordinates s and r. Next assume that the field point \mathbf{x}' lies in the direction such that $\mathbf{x}'-\mathbf{x}_0$ is coplanar with the ray direction \mathbf{n} and the surface normal \mathbf{a}_3 at \mathbf{x}_0 and makes the angle θ_0 with the surface normal. Thus, the field point is exactly in the "launching direction." Near the launch point we have, from (46),

$$|\mathbf{x} - \mathbf{x}'| = R' - s \sin \theta_0 + (1/2R')(r^2 + s^2 \cos^2 \theta_0)$$

$$+ \frac{1}{2} \cos \theta_0 \left(\frac{s^2}{R_{\parallel}} + \frac{r^2}{R_{\perp}} + \frac{2sr}{R_{\perp}} \right) + \cdots$$
 (78)

We assume that the phase of the membrane wave has the paraxial approximation

$$\phi = k[s + \frac{1}{2}\cot\theta_0(r^2/R_D)], \tag{79}$$

where R_D defines the local curvature of the membrane wave front on S. Combining Eqs. (77)–(79) and approximating the preexponential functions by their values at the launch point yield

$$p(\mathbf{x}') \approx \omega k_f 2 \cos \theta_0 Z_s FVG(\mathbf{x}_0, \mathbf{x}')$$

$$\times \int ds \, dr \exp\left[\frac{i}{2} k_f \cos \theta_0 \left[\left(\frac{1}{R_{\parallel}} + \frac{\cos \theta_0}{R'}\right) s^2 + \left(\frac{1}{R_{\perp}} + \frac{1}{R_D} + \frac{\sec \theta_0}{R'}\right) r^2 + \frac{2sr}{R_D} \right] \right]. \tag{80}$$

The integral can be performed in general, but we only consider the case for which the field point is in the far field $(R' \rightarrow \infty)$, so that the result simplifies to

$$p(\mathbf{x}') = -4\pi \frac{c}{R_0} \frac{Z_m Z_s}{Z_m + Z_s} V(\mathbf{x}_0) \left(\frac{1}{R_I R_{II}} + \frac{1}{R_{II} R_D} \right)^{-1/2} G(\mathbf{x}_0, \mathbf{x}'),$$
(81)

where F has been eliminated using (57).

F. Summary of the coupling and launching

A plane wave excites a longitudinal or shear membrane wave of the form given in Eq. (55). The phase $\phi(s)$ is determined from Eqs. (67), (69), and (71), where s=0corresponds to the coupling point at which the Snell condition of Eq. (48) is satisfied. The ray path on the shell surface is found from the modified geodesic equation (65) (rays are geodesics iff c is constant). Finally, the ray amplitude, V(s), is determined by quadrature from Eq. (73). The explicit, high frequency limit of this integral for large s, i.e., at points far from the coupling point, is given by Eq. (75), where P_0 is the incident pressure at the coupling point. The general formula (73) describes the growth of V(s) from nothing to its ultimate value, (75).

The launching or decoupling mechanism is summarized in Eq. (81). Here, G is the 3-D Green's function, $V(\mathbf{x}_0)$ is the amplitude of the launching membrane wave at the launch site x_0 , and R_D is its surface wave-front curvature. Both the coupling and the decoupling depend upon the impedances Z_m and Z_s of Eq. (7). They also depend upon the local radius of curvature in the ray direction, R_{\parallel} of Eq. (47a), and on the "effective" radius of curvature for the membrane wave, R_0 defined in Eq. (58).

These elements can be combined to determine the response in the fluid caused by a membrane wave that travels over a finite length on the surface, created at one point and launched at another. The wave-front curvature R_D at the latter point then depends in a deterministic way upon the initial conditions at the coupling point. Assuming for simplicity that the speed is locally constant at the point of detachment, it follows from Eq. (79) that

$$1/R_D = \tan \theta_0 [A'(s)/A(s)],$$
 (82)

where A(s) and A'(s) come from Eq. (67) subject to the initial conditions (71) at the coupling point. We can then find an expression for the radiated pressure in terms of the parameters at the coupling point, from Eqs. (75) and (81). Let x_1 and x_2 designate the coupling and launch points, respectively, and consider the incident pressure to originate from a point source at x', with the observation point at x, both points in the fluid and in the far field. Then we have

$$p(\mathbf{x}) \approx 4\pi \sqrt{2\pi} \frac{e^{-i\pi/4}}{\sqrt{k_f}}$$

$$\times E_1 E_2 \sqrt{R_{\parallel}} \left| \left(\frac{A(s)\cos\theta_0}{R_1 R_{II}} + \frac{A'(s)\sin\theta_0}{R_{\parallel}} \right)^{-1/2} \right|_2$$

$$\times G(\mathbf{x}', \mathbf{x}_1) G(\mathbf{x}_2, \mathbf{x}) \exp\left(i \int_0^s k \, ds\right), \tag{83}$$

where G is the 3-D free-space Green's function and

$$E \equiv \sqrt{Z_s \rho hc} / (Z_m + Z_s) R_0. \tag{84}$$

It is not obvious at all that the expression (83) is reciprocal under the interchange of source and receiver, as was clearly the case for the analogous 2-D expression, Eq. (37). However, under the interchange the initial conditions for A are altered, and now depend upon surface parameters at x_2 , rather than x_1 . The ODE for A is the same as before, but the integration direction is reversed. Armed with these facts, one can then use certain properties of the solutions of the ODE¹⁵ to relate the reciprocal versions of expression (83) and show that it does indeed satisfy reciprocity. The analysis is lengthy, but similar to that of Appendix B.

III. APPLICATIONS

In this section we test the general theory against exact computations for the canonical shells: the infinite cylinder and the sphere. The excitation for both is by plane wave incidence, and therefore the cylinder really behaves in a 2-D manner (the z dependence is algebraic). However, we include it here because the coupling phenomenon is explicitly three dimensional, and involves all of the parameters discussed in the previous section. In particular, both longitudinal and shear waves are possible. Both the cylinder and sphere present degeneracies in the sense that infinite sets of rays need to be taken into account. In the former case the infinite set of helical rays could be treated individually and summed, but we prefer to treat them in a pseudo-2-D manner for simplicity. In this way the analysis is similar to, and borrows much from, that of Sec. I E. The scattered field for the sphere has degeneracies in the backand forward-scattering directions, associated with a ring of coupling points. We consider this degeneracy separately from the more generic case where the ray theory involves only two discrete points—a coupling and a launching point. Among the various canonical tests considered here, the bistatic scattering for the spherical shell is arguably the most general test of the full 3-D ray theory developed in the previous section. It involves all the basic ingredients of the theory, including a nontrivial ray-tube area equation [see Eq. (67)], whereas the cylinder is essentially 2-D with A = const.

A. The cylindrical shell: 3-D

Consider a plane wave incident at angle θ from broadside on an infinitely long circular cylinder (see Fig. 5).

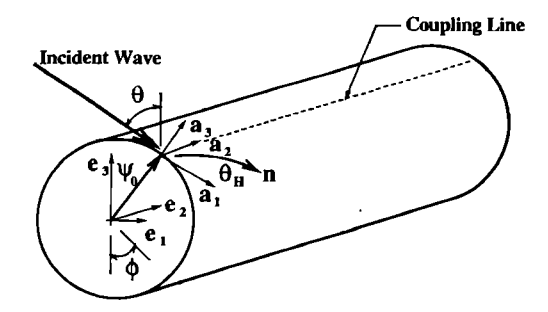


FIG. 5. Coordinate systems used to describe the response of an incident plane wave at angle θ with respect to the axis of an infinite cylinder, the $\mathbf{a}_2 = \mathbf{e}_2$ direction. The ray direction \mathbf{n} and helical angle θ_H are shown. The coupling line given by ψ_0 is also illustrated.

Introduce a right-handed orthonormal triad $\{e_1, e_2, e_3\}$ such that the incident direction is $n^{inc} = -\cos\theta e_1 + \sin\theta e_2$ and e_2 is the axial or z direction (see Fig. 5). The direction of the surface ray, which may be either longitudinal or transverse, follows from Eq. (48). The coupling line is an infinite straight line parallel to the cylinder axis, defined by the angle ψ_0 for which

$$\cos \psi_0 = (\cos \theta_0)/(\cos \theta), \tag{85}$$

where θ_0 is the critical angle, and hence coupling occurs only if $0 \le \theta \le \theta_0$. Consequently, $0 \le \psi_0 \le \theta_0$, with the upper limit being achieved at broadside incidence $(\theta=0)$, whereas $\psi_0=0$ if the incident wave is critical with respect to the axis $(\theta=\theta_0)$. The ray direction and ray normal on S then follow from (48) as $\mathbf{n}=\cos\theta_H\mathbf{e}_\psi+\sin\theta_H\mathbf{e}_2$ and $\mathbf{n}^1=-\sin\theta_H\mathbf{e}_\psi+\cos\theta_H\mathbf{e}_2$, where θ_H , given by either of

$$\sin \theta_H = (\sin \theta)/(\sin \theta_0)$$
 or $\cos \theta_H = (\cos \theta \sin \psi_0)/(\sin \theta_0)$, (86)

defines the helical angle of the ray path with respect to the circumferential direction, and $e_{\psi} = -\sin \psi_0 e_1 + \cos \psi_0 e_3$. We note that the length of one cycle of the helical ray path is $2\pi a \sec \theta_H$.

The principal directions at the coupling point are $e_I = e_{\psi}$ and $e_{II} = e_2$, with principal curvatures $1/R_I = 1/a$ and $1/R_{II} = 0$. The ray-based curvatures of Eqs. (47) are given by

$$\frac{a}{R_{\parallel}} = \cos^2 \theta_H, \quad \frac{a}{R_1} = \sin^2 \theta_H, \quad \frac{a}{R_T} = -\frac{\sin 2\theta_H}{2}. \tag{87}$$

The effective curvatures for longitudinal and transverse waves, defined in (58), may be computed from these expressions. The transverse effective curvature satisfies $1/|R_0| \le 1/a$ with equality when n bisects the directions of principal curvature. This occurs when $\theta_H = \pi/4$, which implies $\theta = \sin^{-1}(c_f/c_i\sqrt{2})$. Figure 6 shows both effective curvatures for steel and water (see Sec. I A for the parameters). The longitudinal and transverse critical angles are 15.82° and 27.21°, respectively, and the maximum for the transverse curvature occurs at $\theta = 18.87$ °.

The far-field scattering amplitude using the ray description can be determined for oblique incidence in much

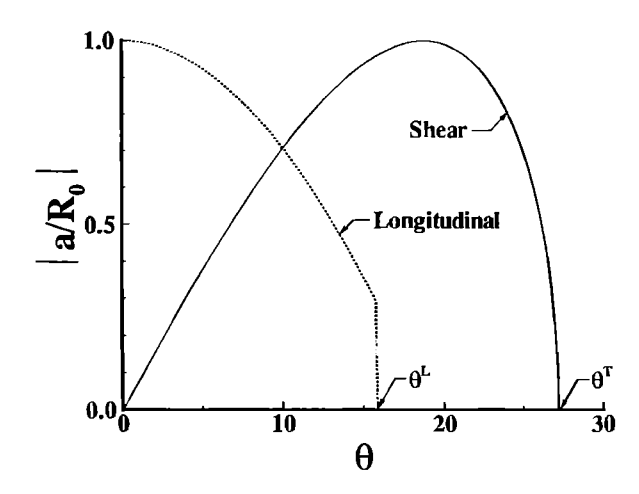


FIG. 6. Effective curvatures for a steel circular cylindrical shell submerged in water.

the same manner as was done for normal incidence in Sec. I. The z dependence, $\exp(ik_z z)$, may be removed from the calculation resulting in one that is essentially 2-D with k_f in (40) being replaced by k_r , of Eq. (92) below (see Appendix A for definitions of related parameters). The same procedure is then followed, and the specularly reflected wave field becomes

$$\hat{p}^{\text{sc}(0)} = P_0 \mathcal{R}(\Psi) [1 + 2r'/(a\cos\psi)]^{-1/2}$$

$$\times \exp[ik_r(r' - a\cos\psi)], \tag{88}$$

where r', Z_f , and \mathcal{R} are given by Eqs. (42), (7), and (15), respectively, and $\Psi = \cos^{-1}(\cos\theta\cos\psi)$ with $2\psi = \pi - \phi$ is the scattered angle (see Fig. 5).

Next, the leaky membrane waves are described along the surface S by Eqs. (55). The pressure in the fluid due to the leakage of the membrane waves traveling on the shell's surface can be determined in much the same manner as that done for the 2-D case. After removing the z component, the relevant wave number entering the Green's function is k_r , and we use \hat{G} to indicate this modification. Then following the same solution procedure outlined for Eqs. (32)–(36), a similar result is obtained for the radiated pressure due to the leaky membrane wave,

$$\hat{p}_{\text{mem}}(\mathbf{x}') \approx V(s) \hat{G}(0,\mathbf{x}') i\omega \frac{\cot \theta_0}{k_f R_0} \frac{2Z_m Z_s}{Z_m + Z_s} \sqrt{\frac{2\pi i k_f a}{\cos \theta_0}},$$
(89)

where Eq. (85) has been used to remove the dependence upon ψ_0 in favor of θ_0 . Recall that R_0 is the radius of curvature for longitudinal or transverse waves (58). Also, V(s) [the analog of V_0 in Eq. (36)] is the launch coefficient of a single ray for the incident plane wave, and follows from (75) and (87) as

$$V(s) = \frac{\sec \theta_H}{-i\omega k_f R_0} \frac{P_0}{Z_m + Z_s} \sqrt{\frac{2\pi i k_f a}{\cos \theta_0}}.$$
 (90)

The coupling from the shell to the fluid can be handled in a manner similar to the 2-D analysis [Eqs. (37)-(39)] with the final result, analogous to Eq. (39), that

$$\hat{p}_{\text{mem}}(\mathbf{x}) \approx \frac{-i4\pi}{k_f a \sin \theta_0} \left(\frac{a}{R_0}\right)^2 \frac{Z_m Z_s}{(Z_m + Z_s)^2} \frac{P_0}{\cos \theta_H} \hat{G}(\mathbf{x}_2, \mathbf{x}) e^{ik_{\phi s} L}.$$
(91)

The azimuthal wave number $k_{\phi s}$ and the radial wave number are determined from

$$k_{\phi s}^2 = k^2 - k_z^2, \quad k_r^2 = k_f^2 - k_z^2,$$
 (92)

with k^2 given by the dispersion relation Eq. (59) and $k_z = k_f \sin \theta$. The ray length L in this calculation is the length of the projection of the helical ray path onto a circle of section, or equivalently, onto the principal curvature direction n₁ on the cylinder. The radiated response generated by the membrane waves can be evaluated in the same manner as done previously for the 2-D problem. Because the response is essentially 2-D, the arclength L traversed by each wave is once again given by the 2-D results of Sec. I but with θ_0 replaced by ψ_0 [see Eq. (44)]. Another way of looking at this is in terms of the phase traveled along a ray from launch to exit, $kL \sec \theta_H$, which contains a z component given as $k_z L \tan \theta_H$. Subtracting the z component of the phase is similar to calculating the distance traveled along the circumferential, n_I, direction on the cylinder and then projecting it into the ray direction. One must take care to retain the complex part of the critical angles in this procedure so that the attenuation is maintained in the phase terms of the membrane scattered wave field.

Having found the radiated response of a single ray of a single species (91), we can now write the total contribution of the leaky membrane waves in a form similar to Eq. (44). Doing so gives, for the membrane wave field,

$$\hat{p}_{\text{mem}} = -P_0 \sum_{\alpha = L, T} \frac{4\pi}{k_{\alpha} a} \frac{Z_m Z_s^{\alpha}}{(Z_m + Z_s^{\alpha})^2} \times \frac{\kappa_{\alpha}^2 \sec \theta_H^{\alpha}}{1 - e^{i2\pi k_{\phi s}^{\alpha} a}} \frac{e^{ik_r(r' - a\cos \psi_0)}}{\sqrt{8\pi i k_r r'}} \times (e^{i2k_{\phi s}^{\alpha} a \left[\pi H(\psi_0^{\alpha} - \psi) + \psi - \psi_0^{\alpha}\right]} + e^{i2k_{\phi s}^{\alpha} a \left(\pi - \psi - \psi_0^{\alpha}\right)}),$$
(93)

where

$$\kappa_{L} = \cos^{2} \theta_{H}^{L} + \nu \sin^{2} \theta_{H}^{L}, \quad \kappa_{T} = \sin 2\theta_{H}^{T},$$
(94)

and the wave numbers k_{α} and $k_{\phi s}^{\alpha}$, the critical angle ψ_{0}^{α} , and the helical angle θ_H^a are determined for each wave type using Eqs. (59), (92), (85), and (86), respectively. The far-field scattering amplitude is determined by evaluating Eq. (40) using Eqs. (88) and (93) along with Eq. (42) to obtain

$$\mathcal{F} = \sqrt{\cos \psi} \mathcal{R}(\Psi) e^{-i2k_{,a}\cos \psi} - \sum_{\alpha:=L,T} H(\theta_0^{\alpha} - \theta)$$

$$\times \frac{4\pi}{k_{,a}a} \frac{Z_m Z_s^{\alpha}}{(Z_m + Z_s^{\alpha})^2} \frac{\kappa_{,a}^2 \sec \theta_H^{\alpha}}{\sqrt{i\pi k_{,f}a}}$$

$$\times e^{-i2k_{,a}\cos \psi_0^{\alpha}} \frac{e^{ik_{,\phi,a}^{\alpha}a(\pi - 2\psi_0^{\alpha})}}{1 - e^{i2\pi k_{,\phi,a}^{\alpha}a}}$$

$$\times \begin{cases} \cos[k_{,\phi,a}^{\alpha}a(\pi - 2\psi)], & \psi > \psi_0^{\alpha}, \\ \cos(2k_{,\phi,a}^{\alpha}a\psi) e^{i\pi k_{,\phi,a}^{\alpha}a}, & \psi \leqslant \psi_0^{\alpha}, \end{cases}$$
(95)

where \mathcal{F} has once again been normalized with respect to the incident wave-field amplitude and a phase shift corresponding to the diameter of the cylinder, and H denotes the Heaviside function. The membrane resonances are again evident, occurring when k_{ϕ}^{α} is close to a whole number in value. Also, the expressions (93) and (95) are clearly discontinuous at $\psi = \psi_0$, and the remarks for the 2-D example of Sec. I E obviously apply here also.

Let us discuss the numerical results. As a check on the accuracy of the asymptotic dispersion relation of Eq. (59), we compared it to that given by the exact solution for a circular cylindrical shell (Appendix A). For a given frequency and angle of incidence θ , the surface wave number k can be calculated from $(ka)^2 = m^2 + (ka)^2$, where m is the complex zero of the denominator in Eq. (A5a). Using a two-term Debye expansion for the cylinder functions of complex order, it was found that the approximation given by Eq. (59) is in very good agreement with the exact surface wave number. For example, at the relatively low value of $k_{f}a = 10$ the largest relative errors in the imaginary parts of the longitudinal and shear wave numbers were 3% and 11%, respectively, for all values of θ below critical. These numbers decreased to $1\frac{1}{2}\%$ and 3% at $k_1a=20$.

The in-surface displacement on the shell depends only upon the coupling mechanism and is independent of the launching. Therefore, as a first check on the accuracy of the coupling, from Eq. (75), we show in Fig. 7 the comparison with the exact theory from Appendix A [Eqs. (A5)]. We note that the ray computations in Fig. 7 involve both longitudinal and shear rays simultaneously. The ray theory is obviously invalid as $k_1 a \rightarrow 0$, but is quite reasonable for $k_f a > 10$. In general, in all the ray results the agreement improves as $k_{\beta}a$ increases. The combined coupling and launching mechanisms are illustrated in the comparisons of the form function in Figs. 8 and 9. We note that the simpler structure in Fig. 8(c) is due to the absence of longitudinal waves. The other figures exhibit the combined influence of both membrane wave types. The nonuniform nature of the ray calculations is evident in Fig. 9(a) at the longitudinal critical angle 15.82°. This could be remedied using transition (erfc) functions, as discussed in Sec. I C.

B. The spherical shell

We now consider a plane wave of unit amplitude incident along the polar axis of a spherical shell, producing a scattered wave field axisymmetric with respect to the polar

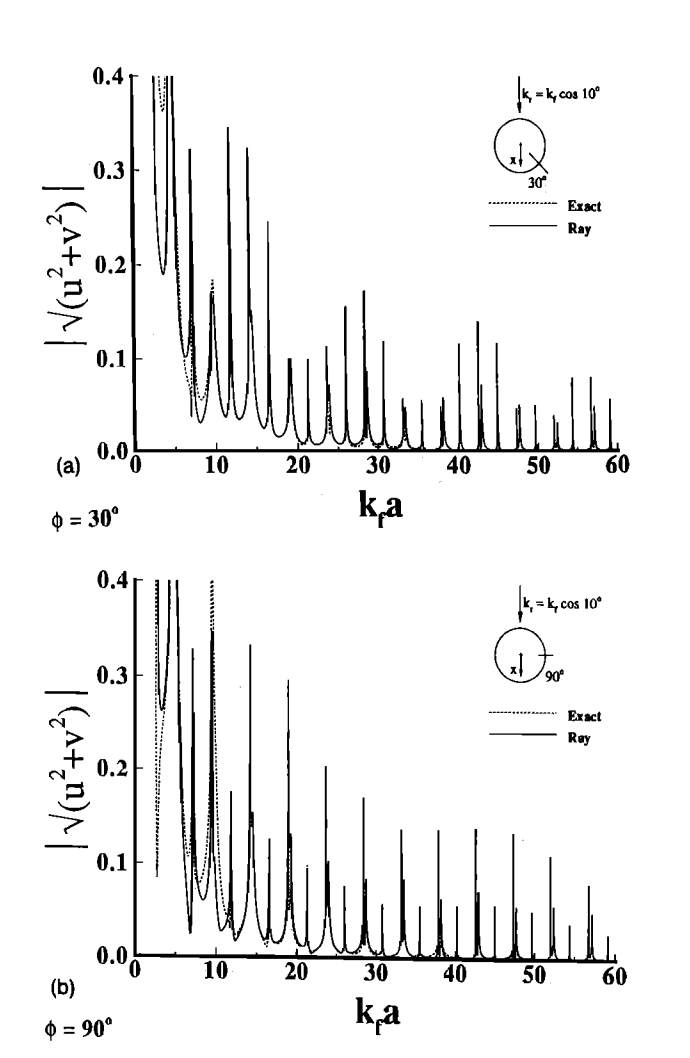


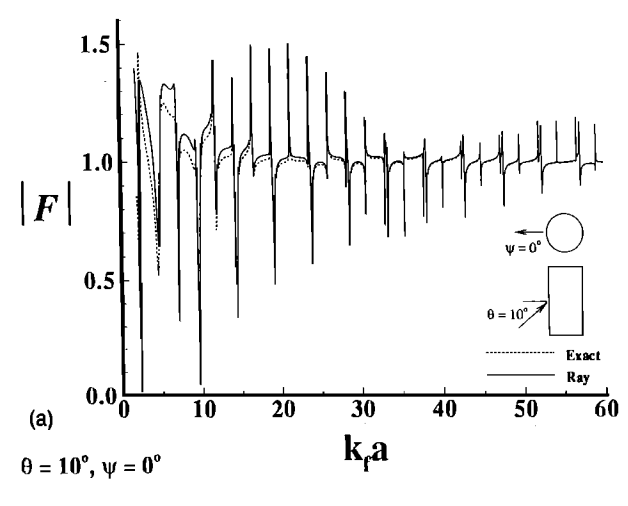
FIG. 7. Comparison of the magnitude of the in-surface displacement at two different positions on the shell, for $\theta = 10^{\circ}$, and (a) $\phi = 30^{\circ}$, (b) $\phi = 90^{\circ}$.

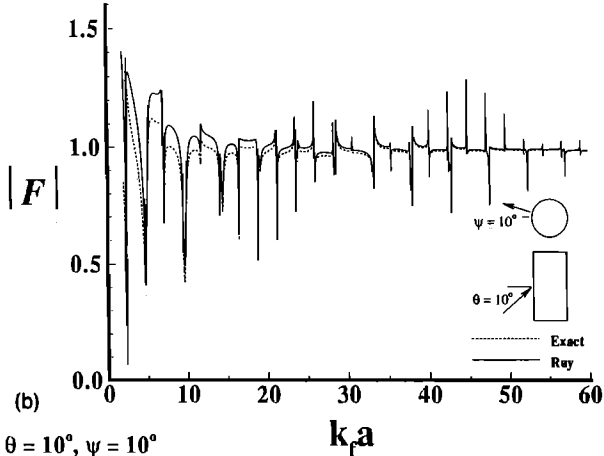
axis. Two distinct situations arise in calculating that part of the field generated by the membrane waves, depending whether the receiver is on the polar axis or off it. In the former case a ring of infinitely many membrane rays radiate from the surface of the sphere toward the observer. But, as the observation point is moved off the polar axis, only two rays contribute to the total wave field and these are shed from the great circle in the plane spanned by the incident and scattering directions. The two situations are obviously different in terms of rays, but could be viewed as limiting cases of a single uniform theory. 10 However, for the sake of simplicity and brevity, we treat the two cases separately. In either case, we note that $1/R_T$ of (47c) and hence $1/R_0$ of (58) both vanish identically everywhere on a sphere, so that there is no coupling to shear waves.

1. Backscatter: receiver on axis

Here we are concerned with determining the backscatter amplitude for the receiver along the polar axis. This case is essentially 2-D because of the axial symmetry. The response in the surrounding fluid caused by the membrane waves can be represented as

$$p_{\text{mem}}(\mathbf{x'}) = 2\pi a^2 \int \left(G \frac{\partial p}{\partial n} - p \frac{\partial G}{\partial n} \right) \sin \theta \, d\theta,$$
 (96)





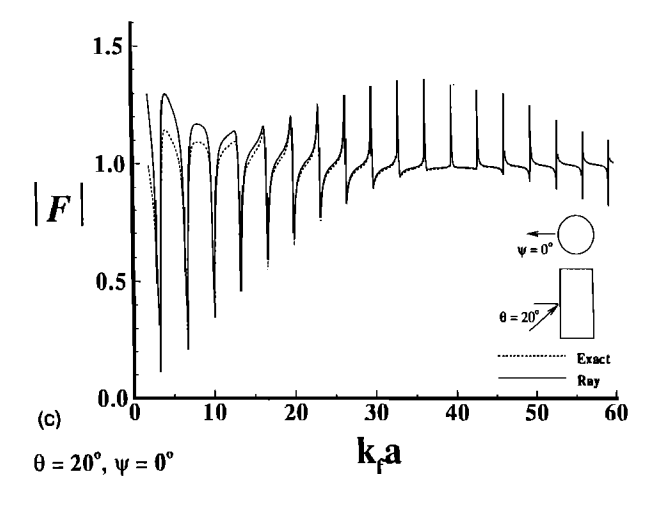
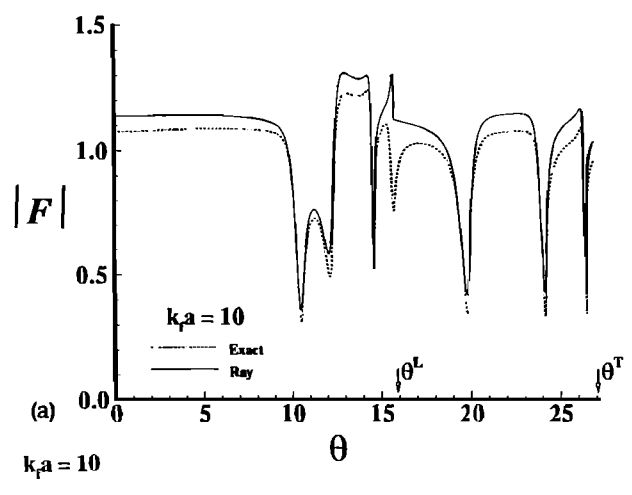
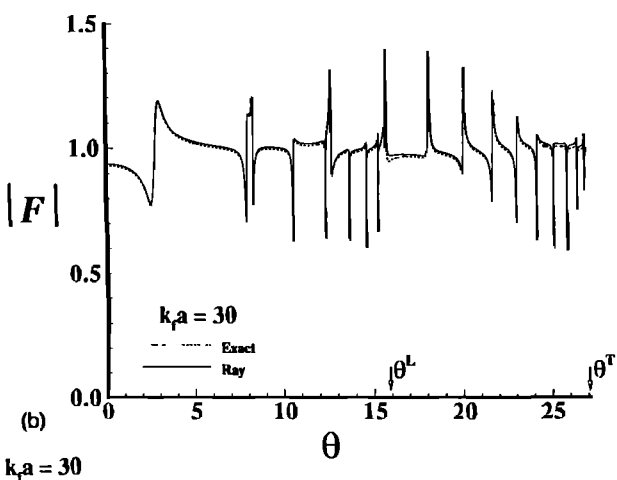


FIG. 8. Comparison of exact and ray-based form functions for a circular cylindrical shell with oblique incidence. (a) $\theta = 10^{\circ}$, $\psi = 0^{\circ}$. (b) $\theta = 10^{\circ}$, $\psi = 10^{\circ}$. (c) $\theta = 20^{\circ}$, $\psi = 0^{\circ}$.

where p is the surface pressure caused by the membrane wave (55), and G is the 3-D free-space Green's function. We note that the surface element is reduced to a single parameter by $dS = 2\pi \sin \theta d\theta$, and that the integral (96) is over any semicircular arc passing through both poles $(\theta=0,\pi)$ (see Fig. 10). The task of evaluating (96) is now formally identical to the 2-D integral considered in Eq. (32). In particular, we assume that the major contribution arises from the vicinity of the ring $\theta = \theta_0$ on the sphere. The





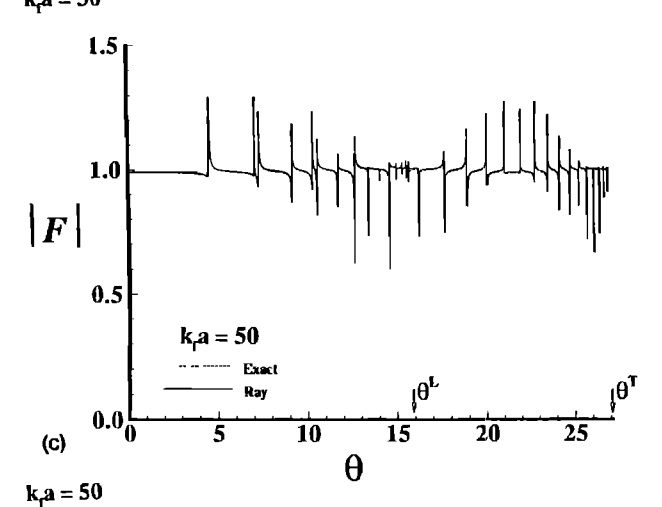


FIG. 9. Comparison of exact and ray-based form functions as the oblique angle of incidence is varied. (a) $k_f a = 10$. (b) $k_f a = 30$. (c) $k_f a = 50$. Note that the ray response is discontinuous at θ^L , the critical angle for longitudinal waves.

phase of the Green's function can be approximated accordingly. Omitting the details, which are the same as for Eqs. (32)-(34), we find that the backscatter is

$$p_{\text{mem}}(\mathbf{x}') \approx 4\pi\omega k_f a^2 Z_s FV(\mathbf{x}_2) \cos\theta_0 G(\mathbf{x}_2, \mathbf{x}')$$

$$\times \int \exp\left(ik_f \cos\theta_0 \frac{s^2}{2a}\right) \sin\theta \, d\theta, \tag{97}$$

where $s=a(\theta-\theta_0)$, x_2 denotes the launch point (ring),

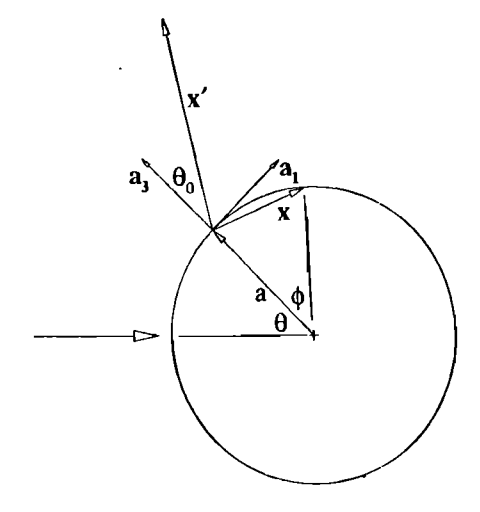


FIG. 10. The spherical shell, coordinate system, source direction, and observation point locations.

and V is the ray amplitude there. We note that

$$\int_{-\infty}^{\infty} \sin(\phi + \theta_0) \exp\left(i\frac{\phi^2}{2}k_f a\cos\theta_0\right) d\phi$$

$$= \sin\theta_0 \sqrt{\frac{2\pi i}{k_f a\cos\theta_0}} \exp\left[-i(2k_f a\cos\theta_0)^{-1}\right], \quad (98)$$

and the final exponential term may be neglected as being asymptotically negligible. Then, using Eq. (57) for the amplitude factor F and Eq. (90) for the ray amplitude coefficient) V, with $R_{\parallel} = R_{\perp} = a$ and $R_0 = a/(1+v)$ in these expressions, Eqs. (97) and (98) reduce to

$$p_{\text{mem}}(\mathbf{x}) = -i8\pi^2 (1+\nu)^2 \frac{P_0}{k_f} \frac{Z_m Z_s}{(Z_m + Z_s)^2} G(\mathbf{x}_2, \mathbf{x}) e^{ikL}.$$
(99)

Here, the possible distance traveled along each ray is $L=2a(\pi-\theta_0)+2\pi am$, m=0,1,2,... In addition, a phase shift of $-\pi/2$ must be included for each time the surface membrane wave passes through either of the two polar focal points on the sphere. These phase shifts are not included in (99).

The total response along the polar axis (axis of symmetry) can then be written in form similar to that for the 2-D cylinder (44). Doing so here gives

$$p_{\text{mem}} = P_0 (1+\nu)^2 \frac{2\pi}{k_f} \frac{Z_m Z_s}{(Z_m + Z_s)^2} \frac{e^{ik_f (R' - a\cos\theta_0)}}{R'}$$

$$\times e^{i2ka(\pi - \theta_0)} \sum_{m=0}^{\infty} e^{im(\pi + 2\pi ka)}, \qquad (100)$$

where the $-\pi/2$ phase factors are due to the membrane wave passing through a focal point once on the first trip around the sphere and twice for every subsequent trip. Also, the incident wave-field amplitude has been phase shifted to the center of the sphere by the amount $k_1 a \cos \theta_0$. Note that $R' \approx R - a \cos \theta_0$, where R is the distance along the polar axis. The far-field backscattering amplitude may be calculated using a relation similar to Eq. (40) but formulated for spherical wave fields as

$$\mathcal{F} = \lim_{R \to \infty} \left[(2R/a)e^{-ik_fR}(p - \hat{p}^{\text{inc}}) \right], \tag{101}$$

where R is measured from the center of the sphere to the far field. One then obtains

$$\mathcal{F} = \mathcal{R}(0)e^{i2k_{f}a} + (1+\nu)^{2} \frac{4\pi}{k_{f}a} \frac{Z_{m}Z_{s}}{(Z_{m}+Z_{s})^{2}}$$

$$\times e^{-i2k_{f}a\cos\theta_{0}} \frac{e^{i2ka(\pi-\theta_{0})}}{1+e^{i2\pi ka}}, \qquad (102)$$

where the surface wave number k is calculated using Eq. (59).

2. Bistatic response: receiver off axis

As usual, the total scattering is split into a specular part and a contribution from the longitudinal shell waves. The specularly reflected wave field for plane wave incidence may be approximated in the far field as^{27,28}

$$p^{\text{sc}(0)} \approx P_0^{\text{sc}}(a/2R')e^{ik_f(R'-a\cos\theta)},$$
 (103)

where P_0^{sc} is given by Eq. (15). In this instance the ray-tube area $[A(R')/A(0)]^{1/2}$ is approximated by 2R'/a. Note that $R' \approx R - a \cos \theta$, where R is the distance in the great circle plane. In order to determine the membrane wave effects, consider the longitudinal ray which begins at s=0, where $s=(\theta-\theta_0)a$. The ray tube area equations [(67) and (71)] are easily solved in this case to give

$$A(s) = (\sin \theta) / (\sin \theta_0). \tag{104}$$

The wave-front curvature becomes, from Eqs. (69) and (79),

$$1/R_D(s) = (1/a)\tan\theta_0\cot\theta. \tag{105}$$

Hence, both the ray tube area and R_D vanish at the poles $(\theta=0,\pi)$ as expected. The scattered field due to a single ray, which couples onto the sphere at $\theta=\theta_0$ and is launched at θ_2 , now follows from Eqs. (83) and (84) as

$$p_{\text{mem}}(\mathbf{x}) \approx P_0 (1+\nu)^2 \frac{4\pi}{k} \sqrt{\frac{2\pi i}{k_f a}} \frac{Z_m Z_s}{(Z_m + Z_s)^2} \times \sqrt{\frac{\sin \theta_0}{\sin (\theta_2 + \theta_0)}} e^{ika(\theta_2 - \theta_0)} G(\mathbf{x}_2, \mathbf{x}).$$
(106)

Note that this becomes singular for $\theta_2 = \pi - \theta_0$ corresponding to the south polar direction for the observer (incidence is from the north polar direction).

We can now write out the total bistatic response in terms of the angle of incidence of the specular ray, θ . The launch angle θ_2 may be expressed in terms of θ and the coupling angle θ_0 . Then combining the clockwise and counterclockwise membrane rays, and using Eq. (106), the total response of the membrane waves becomes

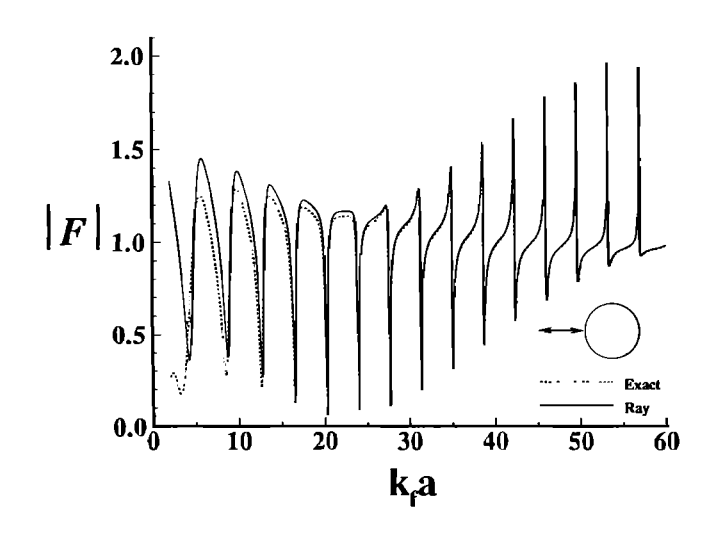


FIG. 11. Comparison of exact and ray-based form functions for back-scatter from a spherical shell. In this instance, the leaky membrane waves form a ring source on the sphere.

$$\begin{split} p_{\text{mem}} &= -P_0 (1+\nu)^2 \sqrt{\frac{2\pi i}{ka \sin 2\theta}} \frac{Z_m Z_s}{(Z_m + Z_s)^2} \\ &\times \frac{e^{ik_f R'}}{k_f R'} \frac{e^{-i2k_f a \cos \theta_0}}{1 + e^{i2\pi ka}} \\ &\times (e^{i2ka[\pi H(\theta_0 - \theta) + \theta - \theta_0]} e^{-i\pi H(\theta_0 - \theta)} - ie^{i2ka(\pi - \theta - \theta_0)}). \end{split}$$

Again, H denotes the Heaviside function, and the phase shifts $-\pi/2$ for each passage through a pole (north or south) have been included. Finally, the form function for bistatic scattering is calculated using Eqs. (101), (107), and (103), giving

$$\mathcal{F} = \mathcal{R}(\theta)e^{-i2k_fa\cos\theta}$$

$$-\frac{(1+v)^2}{k_fa}\sqrt{\frac{8\pi i}{ka\sin 2\theta}}\frac{Z_mZ_s}{(Z_m+Z_s)^2}\frac{e^{-i2k_fa\cos\theta_0}}{1+e^{i2\pi ka}}$$

$$\times (e^{i2ka[\pi H(\theta_0-\theta)+\theta-\theta_0]}e^{-i\pi H(\theta_0-\theta)}-ie^{i2ka(\pi-\theta-\theta_0)}),$$
(108)

where the surface wave number k again follows from Eq. (59).

3. Numerical results

The backscatter comparison with the exact theory from Appendix C is shown in Fig. 11, and an example of bistatic scattering is given in Fig. 12. The asymptotic theory appears to predict the resonance amplitudes well. The discrepancies in the background response between resonances is again attributable to the simplicity of model used for the background field. The deviations of the positions of the resonances in Fig. 11 are more interesting and illustrate how the asymptotic dispersion relation of Eq. (59) fails as $k_f a \rightarrow 0$. If the term $(1-\nu)/R_I R_{II}$ is omitted from the dispersion relation, we find that the disagreement between the exact and approximate resonance dips is larger than shown

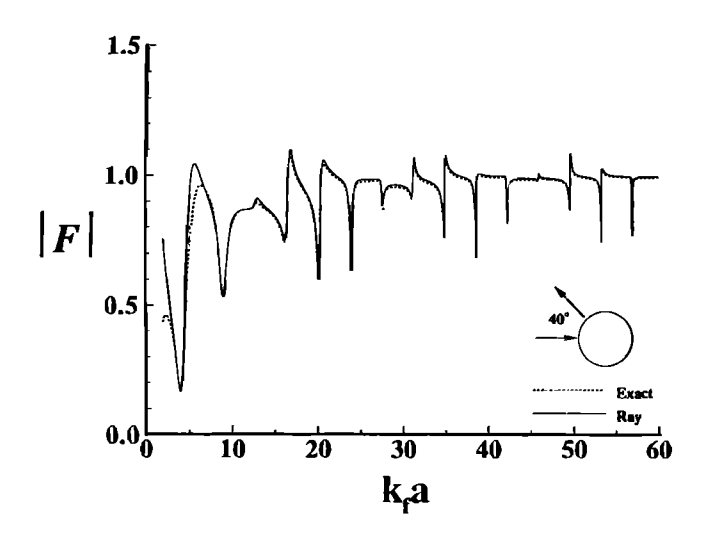


FIG. 12. The exact and ray-based form functions for bistatic response from a spherical shell. Here only two leaky membrane waves contribute and they lie on a great circle in the plane spanned by the incident and scattered directions.

in Fig. 11. However, even though the dispersion may be incorrect, the coupling is still very accurate.

IV. CONCLUSION

Our main results are the diffraction, or coupling, coefficients for membrane waves. The general procedure for applying these coefficients to a practical 3-D scattering configuration is summarized in Sec. II F. The coupling coefficients, combined with ray equations for the membrane waves on the shell, provide the necessary ingredients for developing a ray-theoretic description of acoustic scattering from fluid-loaded shells. Of course, the full strength of ray theory is its applicability to arbitrarily curved, smooth shells. The comparison tests in Sec. III for the separable geometries, the cylinder and sphere, indicate that the ray methods developed here would be suitable for other smooth shell geometries. The present results also show how the midfrequency response for smooth shells can be separated into a "background" response, plus the membrane wave field. The former depends on the shell inertia and the latter on the shell membrane stiffnesses, but not the bending stiffness. In fact, the approximate results reported here are completely independent of the flexural properties of the shell.

ACKNOWLEDGMENTS

This work was supported by the Office of Naval Research under the supervision of Dr. G. Main.

APPENDIX A: THE CYLINDRICAL SHELL

Consider an obliquely incident plane wave of unit amplitude striking a circular cylinder at angle θ from broadside²⁹ (see Fig. 5). The incident and scattered acoustic pressures are

$$(p^{\text{inc}},p^{\text{sc}}) = e^{ik_z z} \sum_{m=0}^{\infty} (A_m J_m(k_r r), P_m H_m(k_r r)) \cos m\phi,$$
(A1)

where J_m and H_m are the *m*th-order Bessel function and Hankel function of the first kind, respectively, and $A_0=1$, $A_m=2i^m$, $m\geqslant 1$. The axial and radial wave numbers are $k_2=k_f\sin\theta$ and $k_r=k_f\cos\theta$ [see Eq. (92)]. The constants P_m are determined from the boundary conditions for a thin circular cylindrical shell³⁰:

$$u_{,zz} + \frac{1 - v}{2a^2} u_{,\phi\phi} + \frac{1 + v}{2a} v_{,z\phi} + \frac{v}{a} w_{,z} + k_p^2 u = 0, \tag{A2a}$$

$$\frac{1+\nu}{2a}u_{,z\phi} + \frac{1-\nu}{2}v_{,zz} + \frac{1}{a^2}v_{,\phi\phi} + \frac{1}{a^2}w_{,\phi} + k_p^2v = 0,$$
 (A2b)

$$\frac{v}{a}u_{,z} + \frac{1}{a^2}v_{,\phi} + \frac{1}{a^2}w + \beta^2 \left(a^2w_{,zzzz} + 2w_{,zz\phi\phi} + \frac{1}{a^2}w_{,\phi\phi\phi\phi}\right) - k_p^2w = -\frac{p}{C},$$
(A2c)

plus the continuity equation [Eq. (6)] evaluated on r=a. In the above, k_f is the fluid wave number, $k_p=\omega/c_p$ is the plate wave number, ν is Poisson's ratio, $C=\rho hc_p^2$, the radius is a, and $\beta^2=h^2/12a^2$.

The above partial differential equations can be reduced to algebraic ones by assuming that the displacements have the form

$$\begin{bmatrix} u \\ v \\ w \end{bmatrix} = e^{ik_z^2} \sum_{m=0}^{\infty} \begin{cases} U_m \cos m\phi, \\ V_m \sin m\phi, \\ W_m \cos m\phi. \end{cases}$$
(A3)

After substitution of Eqs. (A1) and (A3) into Eqs. (A2), one obtains the matrix system

$$\begin{bmatrix} \Omega^{2} - \xi^{2} - [(1-\nu)/2]m^{2} & [(1+\nu)/2]m\xi & \nu\xi \\ [(1+\nu)/2]m\xi & \Omega^{2} - [(1-\nu)/2]\xi^{2} - m^{2} & -m \\ \nu\xi & -m & \Omega^{2} - 1 - \beta^{2}(\xi^{2} + m^{2})^{2} \end{bmatrix} \begin{bmatrix} \dot{U}_{m} \\ iV_{m} \\ iW_{m} \end{bmatrix} = \begin{bmatrix} 0 \\ 0 \\ iG_{m} \end{bmatrix}, \tag{A4}$$

where $\Omega = k_p a$, $\xi = k_a a$, and $G_m = a^2 [A_m J_m(k_\mu a) + P_m H_m(k_\mu a)]/C$. The dispersion relation for the cylindrical shell is given by the vanishing of the determinant in Eq. (A4). To determine the coefficient P_m , first solve for U_m and V_m in terms of W_m . Then, use the w equation of Eq. (A2c) and the continuity equation [Eq. (6)] to solve for P_m . Doing so yields

$$P_{m} = -\frac{k_{r}aE_{m}(\xi)J'_{m}(k_{r}a) - \eta\Omega^{2}J_{m}(k_{r}a)}{k_{r}aE_{m}(\xi)H'_{m}(k_{r}a) - \eta\Omega^{2}H_{m}(k_{r}a)}A_{m},$$
(A5a)

$$U_{m} = \frac{2}{\pi} \frac{\xi}{k_{f}^{2} a} \frac{\eta \Omega^{2}}{D_{m}(\xi)} \frac{[(1-\nu)/2]m^{2} + \nu \{\Omega^{2} - [(1-\nu)/2]\xi^{2} - m^{2}\}}{k_{f} a E_{m}(\xi) H'_{m}(k_{f} a) - \eta \Omega^{2} H_{m}(k_{f} a)} A_{m}, \tag{A5b}$$

$$V_{m} = \frac{2i}{\pi} \frac{m}{k_{f}^{2} a} \frac{\eta \Omega^{2}}{D_{m}(\xi)} \frac{\nu[(1-\nu)/2]\xi^{2} + \Omega^{2} - \xi^{2} - [(1-\nu)/2]m^{2}}{k_{f} a E_{m}(\xi) H'_{m}(k_{f} a) - \eta \Omega^{2} H_{m}(k_{f} a)} A_{m}, \tag{A5c}$$

where the prime indicates differentiation with respect to the argument. Here, $\eta = \rho_f a/\rho h$ is the fluid loading parameter, and

$$D_m(\xi) = [\Omega^2 - (m^2 + \xi^2)] \{\Omega^2 - [(1 - \nu)/2] \times (m^2 + \xi^2)\}, \tag{A6a}$$

$$E_{m}(\xi) = \Omega^{2} - 1 - \beta^{2} (m^{2} + \xi^{2})^{2} - \{\Omega^{2} (m^{2} + v^{2} \xi^{2}) - [(1 - v)/2](m^{4} + 2m^{2} \xi^{2} + v^{2} \xi^{4})\}/D_{m}(\xi).$$
(A6b)

APPENDIX B: PHASE-MATCHING CONDITIONS

According to the present theory membrane waves are excited on the shell by the in-phase beating of the incident field (actually, the background field) with the growing membrane waves. The same picture emerges from a Green's theorem representation of the membrane (insurface displacements) waves, using the Green's function for the fluid-loaded shell. This can be defined for our purposes as the Green's function for the in-surface shell equations, Eq. (53a), without the coupling to w, the latter effect being viewed as a forcing term for the generation of the membrane waves. The difficulty in this approach is that the Green's function is itself difficult to evaluate: however, we may approximate it using ray theory, as follows. First, the Green's function is composed of both types of membrane waves, each of which is defined by an amplitude and a phase. The amplitude functions must decay with distance from the source (along a ray, of course) like $1/\sqrt{A_G(s)}$, where the initial conditions for the ray tube area A_G are

$$A_G(0) = 0, \quad A'_G(0) = 1$$
 (B1)

(in this appendix we take c=const for simplicity). The paraxial approximation to the phase function is of the same form as Eq. (69) with the replacement $A \rightarrow A_G$.

Now consider the membrane wave field at the point x on S caused by coupling in the vicinity of the point x_0 to one particular wave type, longitudinal or shear. Let s_0 be the ray length between the two points, and redefine the origin of s at x_0 , rather than at x. Define $B(s) = A_G(s_0 - s)$. The field at x can then be expressed as an integral of the forcing function, with phase $\phi^{\rm inc}$ given by Eq. (49) (with M=0), multiplied by the membrane Green's function. The phase terms, and the dependence upon the ray distance s_0 , are contained in the integral

$$\int \frac{ds \, dr}{\sqrt{B(s)}} \exp\left[\frac{i}{2}k \cot \theta_0 \left(\frac{s^2}{R_{\parallel}} + \frac{r^2}{R_1} + \frac{2sr}{R_T}\right) - r^2 \tan \theta_0 \frac{B'(s)}{B(s)}\right],\tag{B2}$$

where the final term in the phase is due to the Green's function, and uses the identity $B' = -A'_G$. The integral may then be evaluated by approximating B and its derivative by their values at s=0, yielding a quantity proportional to

$$\left(\frac{B(0)\cot\theta_0}{R_1R_{II}} - \frac{B'(0)}{R_{\parallel}}\right)^{-1/2}$$
 (B3)

This compares with the quantity

$$\left(\frac{A(s_0)}{R_{\parallel}}\right)^{-1/2} \tag{B4}$$

obtained from the analysis leading up to and including Eq. (75). The distinction between these alternative and apparently different results is that (B4) depends upon $A(s_0)$, which has the initial conditions (71), whereas $B(0) = A_G(s_0)$ in (B3) satisfies the initial conditions of (B1). The connecting link is the fact that both A and B solve the same evolution equation, Eq. (67). Also, the remaining parameters in (B3) and (B4) are all defined at the coupling point s=0.

The equivalence follows using the fact that the Wronskian formed from any two solutions of the ray tube evolution equation is a ray constant. Thus, A(s)B'(s)-A'(s)B(s) is independent of s. Equating the Wronskian at s=0 and $s=s_0$ and using the end conditions (71) and (B1) give the desired result that (B3) and (B4) are indeed the same. More generally, if one leaves the initial condition A'(0) as a free parameter, and assumes the general form (72), with R_A and R_B also free, then the same arguments, and the independence of B(0) and B'(0), imply that R_A , R_B , and A'(0) must be assigned the values stated, i.e., $R_A=R_{\parallel}$, $R_B=R_{\parallel}R_{\parallel}/R_{\parallel}$, and $A'(0)=\cot\theta_0R_{\parallel}/R_{\parallel}R_{\parallel}$. Hence, the phase matching conditions as given are unique and unambiguous.

APPENDIX C: THE SPHERICAL SHELL

Consider an incident plane wave of unit amplitude propagating in the direction θ =0 in spherical polar coordinates. The incident and the scattered pressures can be expanded as

$$\frac{p^{\text{inc}}}{p^{\text{sc}}} = \sum_{m=0}^{\infty} P_m(\cos\theta) \begin{bmatrix} A_m j_m(k_f r), \\ D_m h_m(k_f r), \end{bmatrix}$$
(C1)

where j_m and $h_m = h_m^{(1)}$ are the *m*th-order spherical Bessel and Hankel functions, P_m are the Legendre polynomials, $A_m = (2m+1)i^m$, and

$$D_{m} = -\frac{k_{f} a E_{m} j'_{m}(k_{f} a) - \eta \Omega^{2} j_{m}(k_{f} a)}{k_{f} a E_{m} h'_{m}(k_{f} a) - \eta \Omega^{2} h_{m}(k_{f} a)} A_{m}.$$
 (C2)

The fluid-loading parameter η is defined in Appendix A and

$$E_{m} = \Omega^{2} - \beta^{2} \Omega_{m}^{2} (\Omega_{m}^{2} + 1 - \nu) - (1 + \nu)^{2} \frac{(\Omega_{m}^{2} + 1 - \nu)}{(\Omega^{2} - \Omega_{m}^{2})}$$

$$-2(1 + \nu), \qquad (C3)$$

where the membrane modal frequencies are $\Omega_m^2 = m(m+1) - 1 + \nu$, m = 1, 2, 3, ...

- ¹N. D. Veksler, "Intermediate background in problems of sound wave scattering by elastic shells," Acustica 76, 1-9 (1992).
- ²J. D. Kaplunov, E. V. Nolde, and N. D. Veksler, "Asymptotic description of the peripheral waves in scattering of a plane acoustic wave by a spherical shell," Acustica 76, 10-19 (1992).
- ³G. C. Gaunaurd and M. F. Werby, "Sound scattering by resonantly excited, fluid-loaded, elastic spherical shells," J. Acoust. Soc. Am. 90, 2536-2550 (1991).
- ⁴M. F. Werby, "The acoustical background for a submerged elastic shell," J. Acoust. Soc. Am. **90**, 3279–3287 (1991).
- ⁵G. C. Gaunaurd, "Hybrid background coefficients to isolate the resonance 'spectrograms' of submerged shells," J. Acoust. Soc. Am. 92, 1981–1984 (1992).
- ⁶A. Norris and N. Vasudevan, "Acoustic wave scattering from thin shell structures," J. Acoust. Soc. Am. 92, 3320-3336 (1992).
- ⁷ V. A. Borovikov and N. D. Veksler, "Scattering of sound waves by smooth convex elastic cylindrical shells," Wave Motion 7, 143-152 (1985).
- ⁸L. B. Felsen, J. M. Ho, and I. T. Lu, "Three-dimensional Green's function for fluid-loaded thin elastic cylindrical shell: Formulation and solution," J. Acoust. Soc. Am. 87, 543-553 (1990); Errata, 89, 1463-1464 (1991).
- ⁹L. B. Felsen, J. M. Ho, and I. T. Lu, "Three-dimensional Green's function for fluid-loaded thin elastic cylindrical shell: Alternative representations and ray acoustic forms," J. Acoust. Soc. Am. 87, 554-569 (1990).
- ¹⁰ J. M. Ho and L. B. Felsen, "Nonconventional traveling wave formulations and ray-acoustic reductions for source-excited fluid-loaded thin elastic spherical shells," J. Acoust. Soc. Am. 88, 2389–2414 (1990).

- ¹¹ P. L. Marston, "Geometrical and catastrophe optics methods in scattering," *Physical Acoustics*, edited by A. D. Pierce and R. N. Thurston (Academic, New York, 1992), Vol. 21, pp. 1-234.
- ¹²E. G. Williams, B. H. Houston, and J. A. Bucaro, "Experimental investigations of the wave propagation from point excitations on thinwalled cylindrical shells," J. Acoust. Soc. Am. 87, 513-522 (1990).
- ¹³ A. D. Pierce, "Waves on fluid-loaded inhomogeneous elastic shells of arbitrary shape," ASME J. Vib. Acoust. 115, 384-390 (1993).
- ¹⁴A. N. Norris and D. A. Rebinsky, "Membrane and flexural waves on thin shells," ASME J. Vib. Acoust., accepted.
- ¹⁵ A. N. Norris, "Rays, beams and quasimodes on thin shell structures," submitted to Wave Motion.
- ¹⁶D. Feit, "High-frequency response of a point-excited cylindrical shell," J. Acoust. Soc. Am. 49, 1499–1504 (1970).
- ¹⁷ A. D. Pierce, "Wave propagation in thin-walled cylindrical shells," Elastic Wave Propagation, edited by M. F. McCarthy and M. A. Hayes (North-Holland, Amsterdam, 1989), 205-210.
- ¹⁸ A. D. Pierce and H.-G. Kil, "Elastic wave propagation from point excitations of a cylindrical shell," ASME J. Vib. Acoust. 112, 399-406 (1990).
- ¹⁹ A. D. Pierce, "Variational formulations in acoustic radiation and scattering," *Physical Acoustics*, edited by A. D. Pierce and R. N. Thurston (Academic, New York, 1993), Vol. 22, pp. 195-371.
- ²⁰G. C. Gaunaurd and M. F. Werby, "Acoustic resonance scattering by submerged elastic shells," Appl. Mech. Rev. 43, 171-207 (1990).
- ²¹ A. P. Kachalov, "The pattern of sound wave scattering on a convex shell," J. Appl. Math. Mech. (PMM) 43, 336-342 (1979).
- ²² A. L. Goldenveizer, J. D. Kaplunov, and E. V. Nolde, "On Timoshenko-Reissner type theories of plates and shells," Int. J. Solids Structures 30, 675-694 (1993).
- ²³ R. H. Tew and J. R. Ockendon, "Multiple scales expansions near critical rays," SIAM J. Appl. Math. 52, 327-336 (1992).
- ²⁴D. G. Crighton, A. P. Dowling, J. E. Ffowcs Williams, M. Heckl, and F. G. Leppington, *Modern Methods in Analytical Acoustics: Lecture Notes* (Springer-Verlag, New York, 1992), pp. 510-523.
- ²⁵ A. E. Green and W. Zerna, *Theoretical Elasticity* (Oxford U.P., London, 1968).
- ²⁶ A. N. Norris, B. S. White, and J. R. Schrieffer, "Gaussian wave packets in inhomogeneous media with curved interfaces," Proc. R. Soc. London Ser. A 412, 93-123 (1987).
- ²⁷ A. D. Pierce, Acoustics: An Introduction to its Physical Principles and Applications (Acoustical Society of America, Woodbury, NY, 1981).
- ²⁸G. A. Deschamps, "Ray techniques in electromagnetics," Proc. IEEE 60, 1022-1035 (1972).
- ²⁹L. M. Lyamshev, "Sound diffraction by an unbounded thin elastic cylindrical shell," Sov. Phys. Acoust. 4, 161-167 (1958).
- ³⁰ M. C. Junger and D. Feit, Sound, Structures, and Their Interaction (MIT, Cambridge, MA, 1986).